Trabajo Fin de Grado

Ingeniería de Tecnologías Industriales

Simulation of a Rogowski coil for plasma current measurement in the SMART tokamak of the University of Seville

Autor: Juan Sánchez Gamino

Tutores: Manuel Toscano Jiménez

Alessio Mancini

Dpto. Física Aplicada III
Escuela Técnica Superior de Ingeniería
Universidad de Sevilla

Trabajo Fin de Grado

Ingeniería de Tecnologías Industriales

Simulation of a Rogowski coil for plasma current measurement in the SMART tokamak of the University of Seville

Autor:

Juan Sánchez Gamino

Tutores:

Manuel Toscano Jiménez

Alessio Mancini

Dpto. de Física Aplicada III

Escuela Técnica Superior de Ingeniería

Universidad de Sevilla

Sevilla, 2022

Proyecto Fin de Carrera: Simulation of a Rogowski coil for plasma current measurement in the SMART tokamak of the University of Seville

Autor: Juan Sánchez Gamino
Tutores: Manuel Toscano Jiménez
Alessio Mancini

El tribunal nombrado para juzgar el Proyecto arriba indicado, compuesto por los siguientes miembros:

Presidente:

Vocales:

Secretario:

Acuerdan otorgarle la calificación de:

Sevilla, 2022

Agradecimientos

En primer lugar, no puedo agradecer suficiente a Manuel Toscano el haberme dado la oportunidad de hacer este trabajo e introducirme al apasionante mundo de las tecnologías de fusión. Es difícil encontrar un docente tan comprometido con una enseñanza estimulante, enriquecedora y prolongada más allá del aula. Lo considero un referente como profesor y como persona, y me alegra saber que siempre contaré con él para lo que necesite.

También quiero darle las gracias a Alessio Mancini, por sus innumerables consejos y por su paciencia y disposición a la hora de resolver cualquier duda que tuviera. Me ha ayudado enormemente a lo largo de estos meses, y sin él no habría podido sacar adelante este trabajo.

A mis amigos, los que han estado conmigo desde que empecé la carrera y los que he tenido la suerte de conocer durante estos cuatro años. Habéis sido un apoyo fundamental y, a pesar de los confinamientos y los kilómetros, os he sentido siempre cerca. Soy muy afortunado de teneros.

A mi hermana, por los trayectos en coche a la universidad cada mañana, por ser mi vía de escape en las tardes de estudio en casa y por aguantar mis tonterías. Gracias por lo compartido y lo que nos queda por compartir.

Y, por supuesto a mis padres, a los que les debo todo lo que soy. Gracias por el apoyo infinito e inquebrantable, por los valores que me habéis transmitido y por enseñarme tanto. Me habéis dado las herramientas con las que todos los días voy labrando mi camino, y por eso mis logros son tan míos como vuestros. Gracias de corazón.

Juan Sánchez Gamino

2022

Resumen

Uno de los grandes retos de la humanidad en este siglo será abastecer la creciente demanda energética mundial prescindiendo al mismo tiempo de la generación con combustibles fósiles, cuyas reservas empiezan a escasear y cuyas emisiones ya están haciendo un daño irreparable al medio ambiente.

La comunidad científica ha apostado con fuerza por la fusión nuclear como alternativa limpia, segura e ilimitada de producción de energía, y aspira en las próximas décadas a disponer de reactores de fusión funcionales y económicamente viables. Para ello será necesario instruir a las próximas generaciones de físicos e ingenieros en el funcionamiento de este tipo de dispositivos.

Con este objetivo en mente, el Grupo de Ciencia del Plasma y Tecnología de Fusión de la Universidad de Sevilla está desarrollando el SMART (SMall Aspect Ratio Tokamak), un tokamak esférico pionero en España y en la Unión Europea que contribuirá a la investigación de la física del plasma, así como a la iniciación de muchos estudiantes e investigadores a las tecnologías de fusión.

Este trabajo se centrará en el desarrollo de un sistema de medición de la corriente del plasma circulante dentro del SMART. Se propondrá el uso de la tecnología de las bobinas de Rogowski, y se comprobará su funcionamiento mediante simulaciones del modelo 3D del SMART, las cuales se llevarán a cabo en ANSYS usando el paquete Maxwell de electromagnetismo. Los resultados servirán para establecer la idoneidad o no de este tipo de bobinas para su implementación en la construcción del tokamak.

Abstract

One of the great challenges facing humanity in this century will be to supply the world's growing energy demand while dispensing with fossil fuel generation, whose reserves are becoming scarce and whose emissions are already causing irreparable damage to the environment.

The scientific community is strongly committed to nuclear fusion as a clean, safe and unlimited alternative for energy production, and aims to have functional and economically viable fusion reactors in the coming decades. This will require training the next generation of physicists and engineers in the operation of such devices.

With this goal in mind, the Plasma Science and Fusion Technology Group at the University of Seville is developing the SMART (SMMall Aspect Ratio Tokamak), the first spherical tokamak in Spain and in the EU, and will contribute to plasma physics research, as well as to the initiation of many students and researchers to fusion technologies.

This work will focus on the development of a current measurement system for the circulating plasma inside the SMART. The use of Rogowski coil technology will be proposed and tested through simulations of the 3D model of the SMART, which will be carried out in ANSYS, using the Maxwell package of electromagnetism. The results will be used to establish the suitability or otherwise of this type of coil for its implementation in the construction of the tokamak.

Index

Tables Index

Figures Index

1 INTRODUCTION

1.1 Motivation for fusion research

The discovery of nuclear reactions and their enormous potential as a source of primary energy was one of the great milestones of 20th century nuclear physics. Among others, two types of reaction are distinguished: fission reactions, in which an atomic nucleus splits into two or more elements of lower atomic weight; and fusion reactions, in which two light nuclei unite to produce an element of higher atomic weight. Although both phenomena were discovered at about the same time, the development of nuclear reactors based on fission proved to be much more feasible and rapidly applicable for power generation than any fusion-based technology, which is why, starting in the second half of the 20th century, the nuclear power plants we know today proliferated.

At the time it was thought that fission energy could be the key to a decarbonized, stable, fossil fuel-independent energy production system capable of meeting the growing demand for energy, but the production of long-lasting radioactive waste and the environmental disasters linked to this technology, as in the case of Chernobyl and Fukushima, have aroused the distrust of a large part of the public and their respective governments, resulting in a detriment to the contribution of nuclear energy to the grid.

Today, the great commitment to decarbonization is being made through renewable energy sources such as solar and wind power, which in the last decade have got to the forefront of clean energy production. In Spain, 60% of installed capacity corresponds to this type of technology, and they have been able to cover more than 40% of the country's daily electricity demand [1]. However, dispensing with conventional generation and basing the electricity system on solar farms and windmills presents a series of problems that are difficult to solve. Among them is the irregularity with which these types of technologies can harness the energy that reaches them, as they are heavily dependent on weather conditions. While this could be solved with batteries that store the surplus energy for its use in periods of low productivity, massive storage capacity would be needed to cover the huge amount of power supplied daily to consumers, which does not seem feasible in the short or medium term. On the other hand, replacing conventional generation with distributed generation means reducing the inertia of the power grid, since this type of technology does not have large rotating masses whose kinetic energy could oppose to variations in frequency [2]. As a result, a more unstable and less reliable electrical system would be obtained.

Faced with these problems, and with climate change urging us to remodel our energy generation system as soon as possible, it would be vital to find a way to produce clean, safe, cheap energy that can be integrated with other renewable energies and is capable of providing stability. The most promising candidate is nuclear fusion. Numerous experiments, including the ITER experimental reactor, are being designed and evaluated around the world to obtain energetically and economically viable fusion reactors in the coming decades. If this can be achieved, the future of a fully sustainable society would be within our reach.

1.2 Fusion reactions

Fusion reactions take place when atomic nuclei unite to produce a heavier nucleus, releasing or absorbing energy. This energy comes from the difference in mass between the reactants and products of the reaction, the magnitude of which can be calculated with the equivalence between mass and energy:

$$E = \Delta m \cdot c^2 \tag{1.1}$$

For energy to be released, the sum of the masses of the light nuclei must be greater than the mass of the resulting nucleus, i.e., their binding energies must be smaller [3]. Therefore, as can be seen in Figure 1.1, fusion reactions with energy release can only be achieved with elements lighter than iron, and preferably very light atoms such as hydrogen.

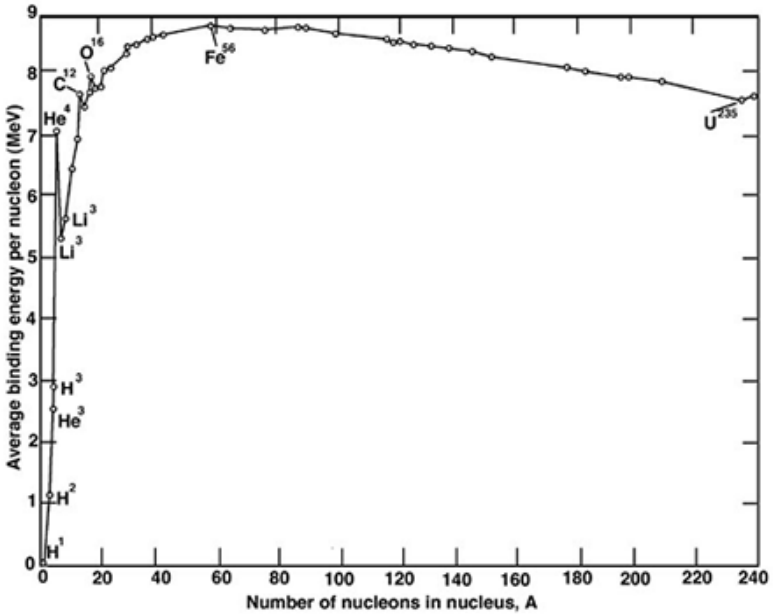

Figure 1.1 Binding energies of elements, reprinted form [4]

On the other hand, for fusion to occur, the nuclei must be able to overcome the electrostatic repulsion between the protons of both nuclei. It is therefore necessary that they are in plasma form and at very high temperature. Thus, the nuclei, separated from their electrons and with high velocity, will be able to collide and get close enough to overcome the so-called Coulombic barrier, beyond which the strong force of the nucleons, which binds protons and neutrons together, becomes dominant over the electrostatic force. The potential energy between the nuclei becomes then negative, as represented in Figure 1.2, and fusion takes place. The temperatures that must be reached for fusion processes are of the order of tens of millions of degrees.

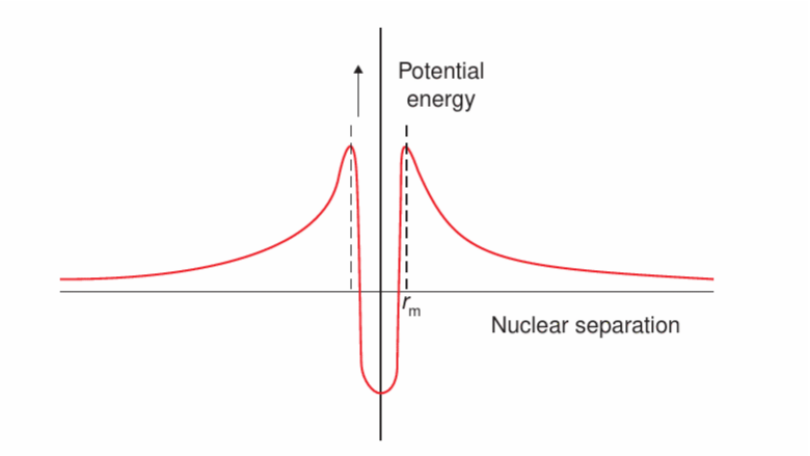

Figure 1.2 Representation of the potential energy of nuclei, reprinted from [3]

There are a multitude of fusion reactions that release energy. The most commonly used in fusion devices is that of two isotopes of hydrogen, deuterium and tritium [3]:

$$ {}^{2}_{1}\mathrm{H} + {}^{3}_{1}\mathrm{H} = {}^{4}_{2}\mathrm{He} + {}^{1}_{0}\mathrm{n} + 17.6\ \mathrm{MeV} \tag{1.2} $$

This reaction is preferred for several reasons. First, it is the reaction that achieves the highest probability of collision at the lowest temperature compared to the other reactions. Secondly, the amount of deuterium available on Earth is practically unlimited, since a good percentage of the hydrogen molecules present in water correspond to this isotope, while tritium, although not so present in nature, can be made from lithium, which is very abundant.

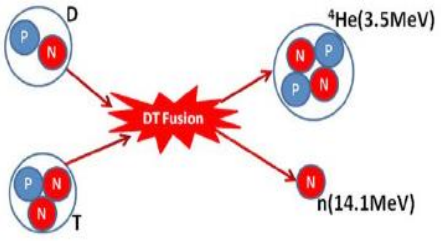

Figure 1.3 D-T Fusion reaction, reprinted from [5]

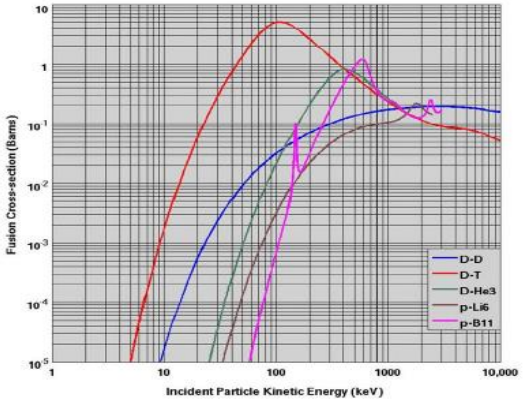

Figure 1.4 Cross-section comparison between different fusion reactions, reprinted from [5]

1.3 Confinement strategies

As mentioned above, very high temperatures and densities are required to achieve fusion. Naturally, if nothing is done to prevent it, the plasma tends to less energetic states that prevent the atoms from reacting with each other. Additionally, the plasma cannot be in touch with the walls of any kind of recipient, as no material can withstand its extreme temperatures. Some sort of confinement is necessary. Various processes are available to confine the plasma so that it can be subjected to fusion conditions for as long as necessary without expanding and cooling.

1.3.1 Gravitational confinement

This is the type of confinement that occurs in stars. Thanks to their enormous mass, stars are able to exert pressure forces on their cores such that the hydrogen trapped in them fuses and releases the energy that keeps it alive. On Earth, however, it is impossible to replicate these mechanical pressure conditions in a sustained manner, so other confinement techniques are necessary.

1.3.2 Inertial confinement

Inertial confinement is based on achieving the required temperature and density for fusion to occur by compressing the hydrogen. To achieve this, a fuel-filled capsule is used, on the surface of which high-energy particle beams or lasers hit. The surface is heated and transformed into plasma, which expands outward and exerts an opposing reaction force on the fuel inside, which is instantly compressed, thus allowing fusion conditions to be reached.

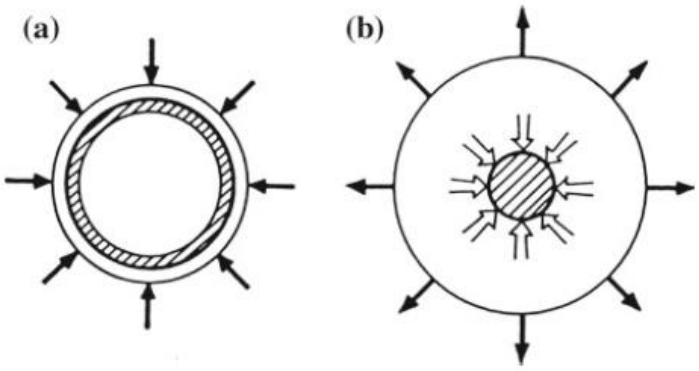

Figure 1.5 Schematic of the implosion of an inertial confinement capsule, reprinted from [6]

This confinement method is used in several of the most cutting-edge devices in fusion research, such as the NIF in the United States and the LMJ in France.

1.3.3 Magnetic confinement

The protons and electrons within the plasma, being unbound from each other, act as charged particles. When subjected to a magnetic field, they experience a force following Lorentz's law,

$$\vec{F} = q \cdot (\vec{v} \times \vec{B}) \tag{1.3}$$

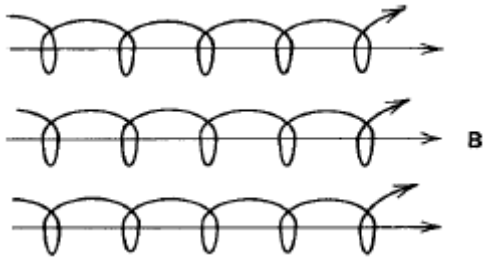

Figure 1.6 Movement of charged particles along magnetic field lines, reprinted from [8]

This principle makes it possible to confine the plasma and force it to flow in a specific region of space as if it were a current thread, away from the walls of the confinement chamber, since the pressure of the magnetic field exerts a pressure on the plasma that counteracts the hot plasma's own natural tendency to expand. This magnetic pressure can be calculated as follows [7]:

$$P = \frac{B^2}{2 \cdot \mu_0} \tag{1.4}$$

Where μ_0 is the magnetic permeability of the vacuum.

The ratio of plasma pressure to magnetic pressure is called the beta coefficient. For confined plasmas, this coefficient is always less than one. [7]

1.3.4 Magnetic confinement devices

Most of the more advanced fusion devices are based on magnetic confinement. The magnetic field is generated by powerful electromagnets, which, to prevent the field lines from leaving the device, are placed around an axis, thus producing closed field lines through which the plasma flows.

Consequently, the curvature of the path causes the particles in the outer part of the plasma to drift towards the walls of the confinement chamber [8]. The need then arises to modify the magnetic field to neutralize these drifts.

Magnetic confinement reactors are classified according to the final shape of the magnetic field inside the device. Two schemes stand out: the stellerator and the tokamak.

1.3.4.1 Stellerator

To counteract the outward drift of the plasma particles, the stellerator coils are designed in such a way that the magnetic field is twisted on its axis, canceling drifts along the torus. This design avoids the need to induce currents in the plasma itself and facilitates working with long duration pulses.

However, it adds difficulties for the manufacturing of the electromagnets, which must be fabricated with a very complex and precise geometry, and the simulations become much more complicated.

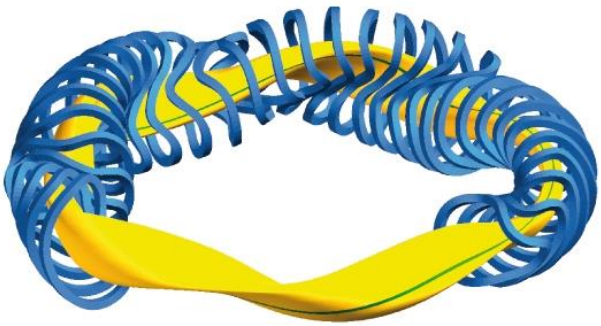

Figure 1.7 Model of the toroidal coils of a stellerator and its generated magnetic field, reprinted from [9]

1.3.4.2 Tokamak

Tokamaks are devices that confine the plasma by means of a toroidal magnetic field generated by a series of flat coils around the confinement chamber.

The fundamental difference with respect to stellerators is the use of the plasma current for confinement purposes. By means of a solenoid in the center of the torus, which acts as the primary of a transformer, a current is induced in the plasma itself, which would be the secondary winding of the transformer, generating around it a poloidal field of the order of 10 times smaller than the toroidal field [3]. This field exerts a centripetal force on the helical trajectory of the plasma particles, compressing it towards the center of the plasma itself.

Thus, the combination of both, one in the direction of the current and the other perpendicular to it, results in a helical field that confines the plasma and counteracts the instabilities due to its curvature.

Additionally, a series of coils, called poloidal field coils, arranged at different heights around the toroid cross section are often added for complementary plasma control and shaping.

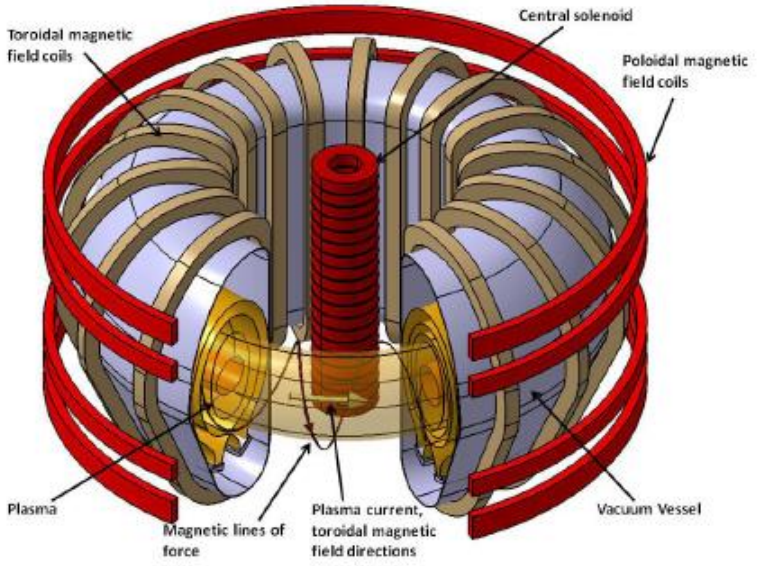

Figure 1.8 Schematic of a tokamak and its coils groups, reprinted from [5]

This strategy lowers the manufacturing and installation costs of the reactor assembly. However, the need to charge and discharge the central solenoid to induce the plasma current makes it difficult to operate the tokamak long enough.

Tokamak characteristic parameters

Each tokamak is defined in first approach by a few parameters that describe some of its geometric and operational characteristics. These are shown in Table 1.1.

Table 1.1 Characteristic parameters of a tokamak

Parameter	Notation	Description
Major radius	R	Distance between the center of the toroid and the center of the plasma
Minor radius	a	Radius of the section of the plasma inside the vacuum chamber
Aspect ratio	R/a	Relation between major and minor radius
Toroidal field	B_t	Magnetic field generated by the toroidal coils
Plasma current	I_p	Current induced in the plasma
Pulse length	τ_p	Amount of time in which the plasma characteristics meet fusion conditions

Spherical tokamaks

The spherical tokamak is a type of tokamak characterized by a lower aspect ratio than conventional tokamaks. This design allows the plasma to be confined more efficiently, i.e., a smaller magnetic field needs to be induced to confine the same amount of plasma [8].

It therefore allows higher beta values to be achieved, and the compactness of its design makes it cheaper than conventional ones. Nevertheless, the space available in the center of the torus for the central solenoid and other devices is significantly reduced. The figure shows a comparison between the cross-section of a spherical tokamak and that of a higher aspect ratio tokamak.

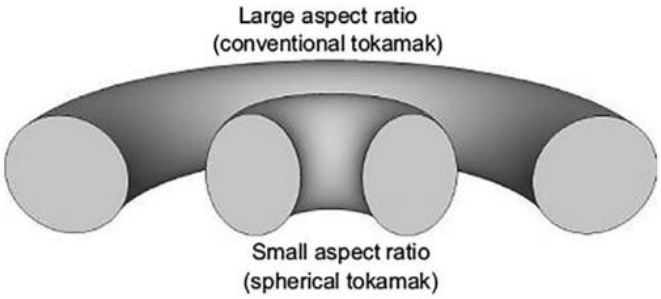

Figure 1.9 Comparison between a conventional tokamak and a spherical tokamak, reprinted from [9]

1.3.5 The SMART Tokamak

The SMART (SMall Aspect Ratio Tokamak) is a fusion device currently being designed by the Plasma Science and Fusion Technology Group, as a collaborative research project between the CNA (Centro Nacional de Aceleradores) and the University of Seville. It is a spherical tokamak (Aspect ratio < 2) that will contribute to fusion research and help train future physicists and engineers in the field. It will have 12 toroidal field coils, 4 pairs of poloidal field coils and a central solenoid. Its operation will be divided into three successive phases that will progressively operate the tokamak up to its maximum capacity. The operational parameters of each of the phases are summarized in the following table.

Table 1.2 Operational parameters of the three phases of the SMART

Parameter	Phase 1	Phase 2	Phase 3
Toroidal field	0.1 T	0.3 T	1 T
Plasma current	30 kA	100 kA	500 kA
Pulse length	20 ms	100 ms	500 ms

1.4 Objectives and scope

The magnetic confinement of a tokamak plasma is a highly complicated procedure and subject to many instabilities. This is why, in order to perform fusion experiments, it is vital to have control systems that monitor in real time the characteristics and evolution of the plasma inside the vacuum chamber.

Throughout this work, the measurement of the plasma current inside the SMART will be studied. The aim is to contribute to the design of a control system based on Rogowski type coils, whose behaviour in different plasma current scenarios will be studied by means of dynamic simulations in ANSYS.

Chapter 2. Rogowski coil basics

Theoretical and practical foundaments of Rogowski coil design and its scope and suitability for fusion applications will be explained, along with examples in already existing tokamaks.

Chapter 3. SMART modelling and simulation in ANSYS

The design of the SMART tokamak of the University of Seville will be presented, explaining the geometrical and material characteristics of each of its components. Subsequently, the finite element analysis, used in ANSYS to solve problems of electromagnetism equations, will be introduced. Finally, the model used in ANSYS for the simulations will be shown, explaining and justifying any simplifications that may have been made.

Chapter 4. Results of the simulations

The results of the simulations will be presented and analysed by comparing them with reference values. Based on the conclusions drawn, the suitability of this type of technology for the task in hand will be discussed.

2 ROGOWSKI COIL BASICS

A Rogowski coil (RC) is an electronic device used for current measurement. They consist of a coil whose axis forms a closed path around the conductor through which the current that wants to be measured passes.

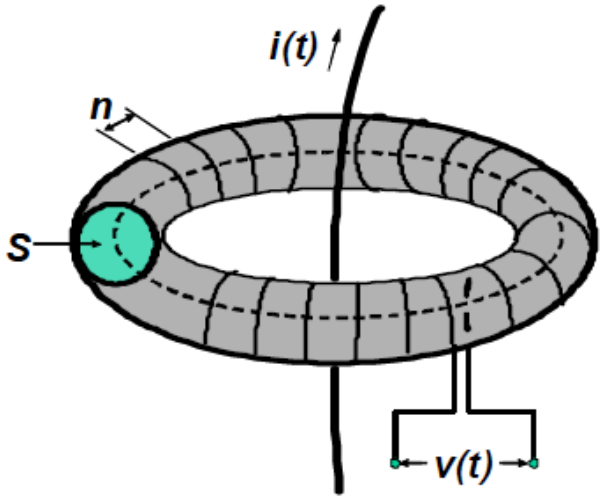

Figure 2.1 Schematic of a Rogowski coil, reprinted from [15]

2.1 Principle of operation

To understand how a RC Works, it is convenient to start with the Maxwell equations and apply them to the characteristics of this type of coil.

Table 2.1 Maxwell equation in differential and integral form

Differential form		Integral form	
$\vec{\nabla} \cdot \vec{E} = \frac{\rho}{\varepsilon_0}$	(3.1)	$\oint_S \vec{E} \cdot d\vec{S} = \frac{q}{\varepsilon_0}$	(3.2)
$\vec{\nabla} \cdot \vec{B} = 0$	(3.3)	$\oint_S \vec{B} \cdot d\vec{S} = 0$	(3.4)
$\vec{\nabla} \times \vec{E} = -\frac{d\vec{B}}{dt}$	(3.5)	$\oint_C \vec{E} \cdot d\vec{l} = -\frac{d}{dt}\int_S \vec{B} \cdot d\vec{S}$	(3.6)
$\vec{\nabla} \times \vec{B} = \mu_0 \cdot \vec{J} + \mu_0 \cdot \varepsilon_0 \cdot \frac{d\vec{E}}{dt}$	(3.7)	$\oint_C \vec{B} \cdot d\vec{l} = \mu_0 \int_S \vec{J} \cdot d\vec{S} + \mu_0 \cdot \varepsilon_0 \frac{d}{dt}\int_S \vec{E} \cdot d\vec{S}$	(3.8)

Consider an ideal RC, with constant cross section A, number of turns N and whose axis forms a circumference of length l around a conductor through which a current I flows. The voltage across the coil is:

$$V_{RC} = N \cdot \oint_C \vec{E} \cdot d\vec{l} \tag{3.1}$$

Being C the loop described by one turn of the RC.

Taking Faraday's law in its integral form (Eq. 3.6), and assuming that the magnetic field does not vary in the RC section, the voltage is as follows:

$$V_{RC} = -N \cdot A \cdot \frac{dB}{dt} \tag{3.1}$$

The Ampère-Maxwell law in integral form (Eq. 3.8) indicates that there is a relationship between magnetic field and the electric current that generates it. Assuming that the Displacement Current term (the second term on the right-hand side of equation 3.8) is negligible, and that the magnetic field remains constant as it passes through the RC axis, it follows that the magnetic field is proportional to the current.

$$B \cdot l = \mu_0 \int_S \vec{J} \cdot d\vec{S} = \mu_0 \cdot I \tag{3.1}$$

Being S the cross-section of the RC. Therefore, by putting equations 3.8 and 3.9 together, we obtain a relationship between the voltage induced in the RC and the current flowing through it:

$$V_{RC} = -M \cdot \frac{dI}{dt} \tag{3.1}$$

Where M is equal to $\frac{N \cdot A \cdot \mu_0}{l}$ and stands for the mutual induction constant between the RC and the conductor.

As seen in equation 3.4, the induced voltage is proportional to the derivative of the current contained in the region bounded by the RC. Therefore, by integrating this voltage signal over time, the evolution of the current can be obtained.

An integrator circuit is used to integrate the signal. A basic integrator consists, as shown in figure 2.2., of a resistor and a capacitor in series.

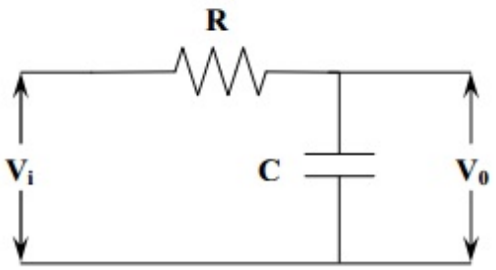

Figure 2.2 Basic integrator circuit, reprinted from [13]

The signal obtained at the output, assuming that the measurement time is much less than the product of R·C [11], is as follows:

$$V_o = \frac{1}{R \cdot C} \cdot \int_0^t V_i dt \quad = \frac{1}{R \cdot C} \cdot \int_0^t \left(M \cdot \frac{dI}{dt} \right) dt \quad = \frac{M}{R \cdot C} \cdot I \tag{3.5}$$

This circuit allows to obtain an output signal that is proportional to the current that is being measured. Normally an operational amplifier is added to the integrator circuit, as shown in Figure 2.4.

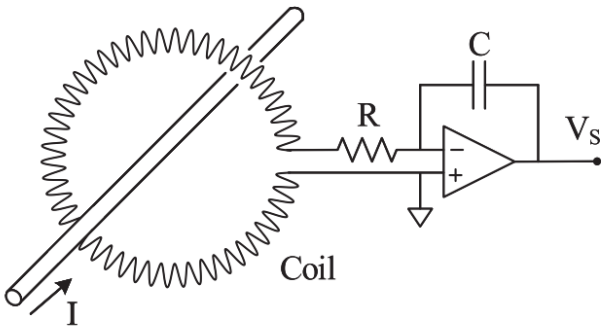

Figure 2.3 RC with integrator, reprinted from [12]

2.2 Properties and constructive aspects of the Rogowski coil

Listed below are the main properties that distinguish the RC:

- **Elimination of saturation.** As the core of RCs is not ferromagnetic, there is no saturation possible, unlike other devices such as current transformers, which do have a ferromagnetic core. Thanks to this property, the operating range of this type of coil is very high, from a few tens of amperes to hundreds of thousands. On the other hand, the mutual inductance between

the conductor and the coil is very small, which makes it necessary to build them with a high number of turns, so that the output voltage is appreciable.

- **Response time**. RCs are usually designed to have a very quick response time [14]. This makes them particularly suitable for applications in which it is intended to measure fast changing currents.
- **Independence of conductor position and coil shape**. The response of a RC is unaffected by changes in the position of the conductor passing through it, provided that the cross-sectional area and number of turns per unit length remain constant. The path around which the RC is wounded is also independent from the mutual inductance, as long as it forms a closed path, so it does not need to form a circumference around the conductor and can therefore be adapted to the device in question.
- **Shielding from external magnetic fields.** Because the RC advances tangentially with a certain pitch at each turn, it forms a helix in space. If this helix is understood as the sum of two coils, one of section A (that of the toroid), and number of turns equal to that of the original RC, and another coil of a single turn of section A' (that of the area enclosed inside the RC and contained in the plane of its axis), corresponding to the tangential advance of the winding, it is easily observable that, in case there are variable magnetic fields in the direction perpendicular to the plane, the induced voltage would be affected, since an electromotive force would be induced in the coil of greater area.

  To counteract this effect, one of the coil terminals is passed through the center of the core, emulating this second virtual coil but connected in the reverse direction, so that the induced voltages cancel each other out (Figure 2.3). Another option is to add a second winding in series with the first but wound in reverse, as shown in Figure 2.4.
- **Flexibility in installation.** Since the core of the Rogowski is not made of a rigid ferromagnetic material, the device can be flexible and adapt to the geometry of the location where it is installed.

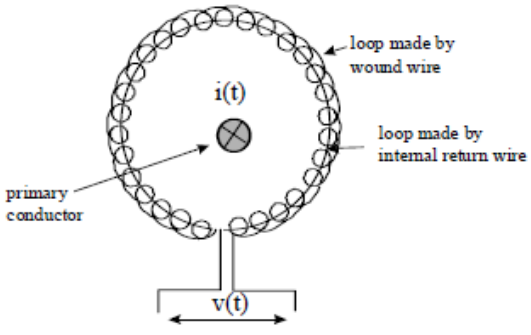

Figure 2.4 Schematic of a RC with return loop, reprinted from [15]

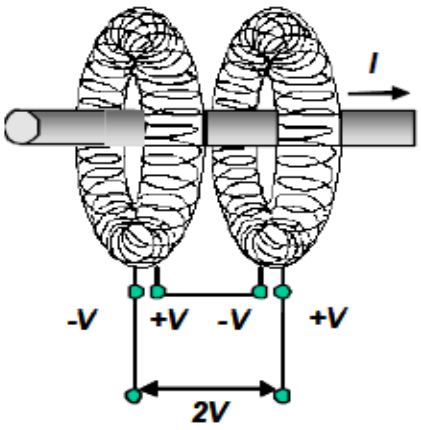

Figure 2.5 RC with two separate inverse windings, reprinted from [15]

Suitability for plasma applications

Many of the components of a tokamak are subjected to high currents during plasma experiments, including the plasma itself. To properly evaluate their behaviour, reliable and versatile current measuring devices with sensitivity to a wide range of current values are necessary, in particular for the plasma, in which, unlike field coils, the current flow is not defined by the limits of a conductor, but is in motion in the vacuum chamber. Knowing the magnitude of its current is of vital importance to study how it evolves throughout the experiment.

Because of the properties listed above, the RC has the necessary qualities for the measurement of the plasma current and other parameters of the SMART.

2.3 Examples of Rogowski coils in Tokamaks

Some of the already existing Tokamaks in the world use the Rogowski technology to measure currents inside them.

2.3.1 The Alvand Tokamak

The Alvand Tokamak is a fusion reactor developed in Tehran, Iran. It was first built in 1975 and has been updated to newer versions two times since: Alvand-IIC in 1980 and Alvand-U in 2004 [16].

Its main features are summarized in the following table.

Table 2.2 Characteristics of the Alvand Tokamak [16]

Parameter	Value
Major radius	0.46 m
Minor radius	0.13 m
Aspect ratio	3.54
Toroidal field	0.8 T
Plasma current	30 kA
Pulse length	10 ms

Its RC is used to measure the plasma current. Its core is made of Teflon and has 3366 turns, with an internal radius of 12.6 cm and an external radius of 13.74 cm. It uses the return loop technique for external field cancellation.

According to [17], it was able to measure with 1% accuracy the evolution of the plasma current during the experiment.

Figure 2.6 Rogowski Coil installed inside the Alvand Tokamak, reprinted from [17]

2.3.2 NSTX (National Spherical Tokamak Experiment)

The NSTX is a spherical tokamak developed by the Princeton Plasma Physics Laboratory. Its first plasma was achieved in 1999 and in 2012 underwent an upgrade to enhance its operational parameters, becoming the NSTX-U [18].

Table 2.3 Characteristics of the NSTX [18]

Parameter	Value
Major radius	0.85 m
Minor radius	0.65 m
Aspect ratio	1.31
Toroidal field	0.3 T
Plasma current	1400 kA
Pulse length	5 s

The NSTX has RCs installed to measure plasma current, eddy currents and Halo currents. Eddy currents are the currents induced in the conductive materials of the Tokamak by the presence of varying magnetic fields. Halo currents occur when the magnetic confinement is not sufficient and the plasma encounters the walls of the vacuum chamber, allowing the current to pass through them. [19]

The material chosen for the plasma current RC was Teflon. Its core has a rectangular shape with curved edges, dimensions 12.2 x 28 mm and a length of 10.36 m for a total of 31416 turns. The return loop was used for protection against external magnetic fields. [20].

Both the Halo current RCs and the eddy current RCs consist of a 19 x 3.75 mm ceramic webbing core, around which 4543 turns of copper wire were wound.

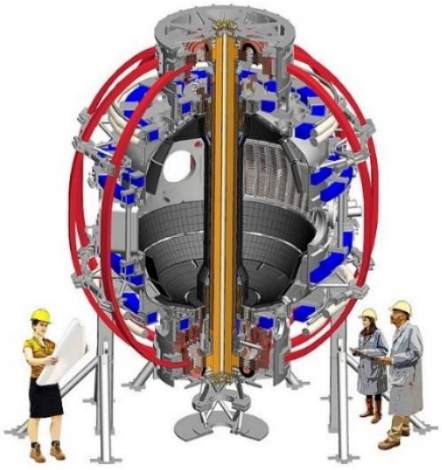

Figure 2.7 Drawing of the NSTX compared to the size of human beings, reprinted form [18]

2.3.3 JET (Joint European Torus)

JET is one of the most prominent Tokamak devices in the world. It is located in Oxford, England, and holds the record for the largest amount of fusion energy produced during by a fusion device, 59 MJ. [21].

Table 2.4 Characteristics of the JET Tokamak [15]

Parameter	Value
Major radius	2.96 m
Minor radius	0.96 m
Aspect ratio	3.08
Toroidal field	3.45 T
Plasma current	5000 kA
Pulse length	5 s

At JET Rogowski coils are used for measuring halo currents. They are integrated in four HCS (Halo Current Sensor). For each HCS, eight RCs are set up to pick up halo currents. They have a cross section of 0.837x0.537 cm. For the cancellation of external magnetic fields, a second inverse winding has been chosen, as can be seen in the right-hand coil of Figure 2.8. [22]

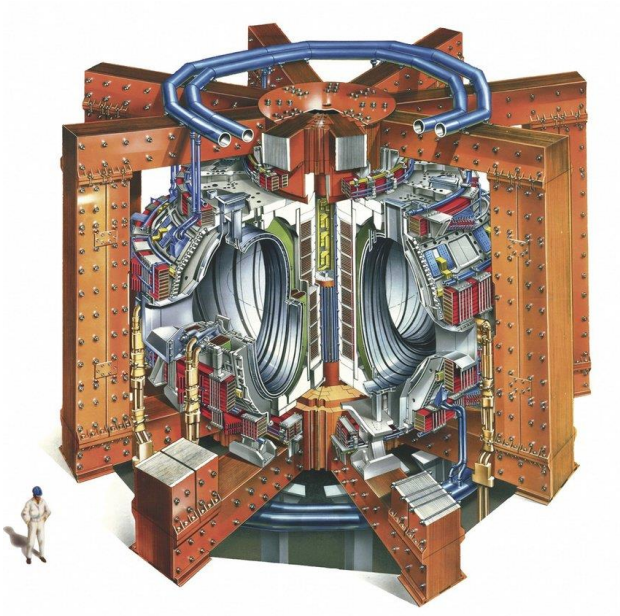

Figure 2.8 Drawing of the tokamak JET, reprinted from [28]

Figure 2.9 Rogowski coils used in JET with their protective case, reprinted from [22]

3 SMART MODELLING AND SIMULATION IN ANSYS

In order to establish many of the design parameters of the SMART, the PSFT Group has resorted to 3D simulations of the SMART. These simulations have been carried out using the ANSYS software, which allows to recreate the conditions that the device will have to withstand during its operation. In this way, for example, the electromechanical loads to which the vacuum chamber will be subjected have been estimated, thus establishing the dimensions it must have in order not to break [26, 27].

This work has also been based on 3D models in ANSYS, but with the aim of studying the behaviour of a RC and its suitability as a method of measuring the plasma current in the SMART.

Throughout this chapter, the steps taken to create the final model of the SMART, including the RC, will be outlined. The geometry and positioning of the Tokamak and coil components will be described in detail, as well as any simplifications that have been made. The finite element method, used by ANSYS to solve Maxwell's equations applied to 3D models, will also be introduced.

3.1 Introduction to ANSYS Maxwell

ANSYS is a software dedicated to the simulation of parts or sets of parts belonging to an engineering product in order to predict their behavior under certain conditions. It is based on the finite element method to solve the differential equations that govern the physics of the model in question.

The finite element method is a numerical technique for solving differential equations. It is applied in various fields of engineering, from fluid mechanics to electromagnetism, since the complexity of the models usually studied does not allow the analytical resolution of their differential equations.

It is based on the subdivision of the object into simpler parts (elements), going from a continuous problem with infinite degrees of freedom to a discretized one with a limited number of degrees of freedom [24]. The geometry of these elements can vary according to the problem [23]. As the equations governing the continuous model are the same as those governing each of the elements, this method makes it possible to solve the equations numerically in the region bounded by each element. The set of all these local solutions results in an approximate solution of the global problem.

ANSYS is responsible for the computational application of the finite element method. The procedure that follows can be divided into three stages [23]:

- **Geometry definition and simplifications.** First of all, the object or set of objects to be simulated must be transferred to ANSYS. To do this, a model is built following the geometric characteristics of each object, including simplifications if necessary.
- **Preprocessing and Mesh generation.** In this stage, the properties of the materials that make up the object are defined in the model and the Mesh is generated. The Mesh is the network of elements into which the object is divided.

- **Resolution.** In this stage, the boundary conditions of the problem are applied, and the system of differential equations is solved. Depending on the shape and the number of elements of the Mesh, the resolution will require a larger computationally effort.
- **Post-processing**. This stage comprises the user analysis of the results with their corresponding graphs, tables, etc.

For this work, the ANSYS Maxwell package has been used, which is used to solve the equations of electromagnetism.

3.2 SMART description

As already mentioned in chapter 1, the SMART is a spherical tokamak developed by the University of Seville in collaboration with the CNA. Its main components are: the vacuum chamber, the toroidal field coils, the poloidal field coils and the central solenoid. The design of all parts has been carried out by the PSFT Group.

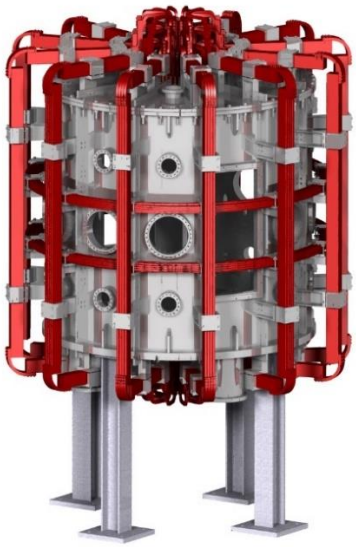

Figure 3.1 External view of the SMART

Figure 3.2 SMART cross-section

3.2.1 Vacuum Vessel

The vacuum chamber is a key component, as it is responsible for ensuring adequate vacuum conditions for plasma experiments and for withstanding high mechanical stresses induced by the powerful magnetic fields induced inside it.

It has a cylindrical shape with a hole in the centre for the central solenoid and the inner arms of the toroidal field coils. It has a height of 1730 mm, an outer radius of 808 mm and an inner radius of 150 mm. The inner wall is 3 mm thick while the outer wall is 8 mm thick. Both the bottom cover and the top cover are 18 mm thick.

3.2.2 Toroidal Field Coils (TFC)

The TFC are the electromagnets responsible for generating the main magnetic field of the tokamak: the toroidal field.

They consist of a total of 12 copper coils arranged around the vacuum chamber, forming a 30° angle between coil and coil. The inner arms of all the coils pass through the central hole. Each coil is made up of four turns. The conductors have a square cross-section of 21.5 x 21.5 mm [25].

3.2.3 Poloidal Field Coils (PFC)

The Poloidal Field Coils are the electromagnets in charge of controlling the shape and positioning of the plasma in the vacuum chamber. They are divided into 4 independent pairs of coils: PF1, PF2, DIV1 and DIV2. Each coil is symmetrically positioned vertically with respect to its corresponding pair and forming a closed path around the main axis of the tokamak. DIV1, DIV2 and PF2 are inside the vacuum chamber, while PF1 is outside the vacuum chamber, as shown in figure 3.1. PF1, PF2 and DIV2 have 23 turns of 10x10 mm copper conductor, while DIV1 has 35 turns of the same conductor. The coordinates of the midpoints of the coils in the vertical plane with respect to the centre of the tokamak are given in Table 3.1.

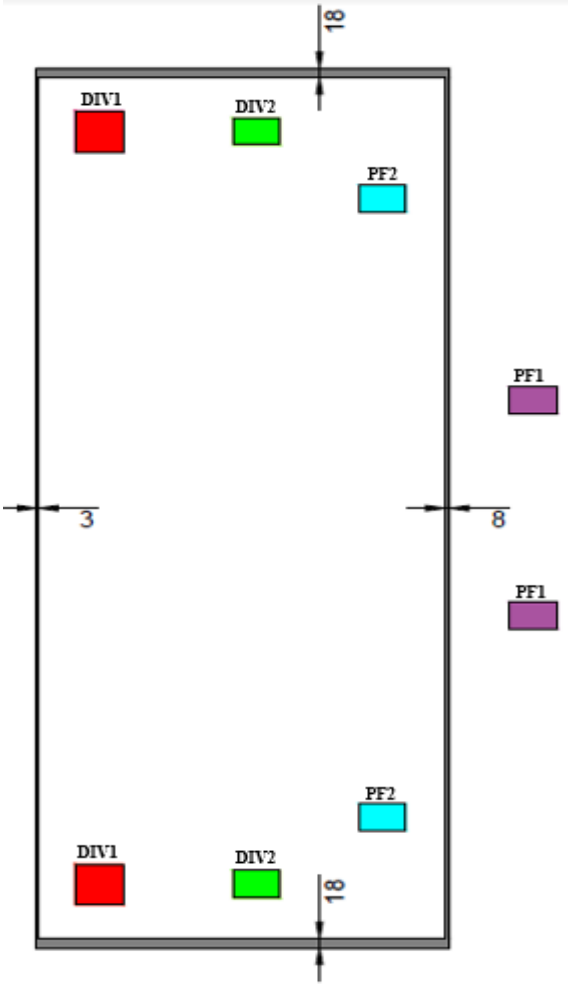

Figure 3.3 Cross section of the vacuum vessel and the PFC

Table 3.1 Positions of the PFC

Coil	Position [mm]
DIV1	(250,±700)
DIV2	(500,±700)
PF1	(940,±200)
PF2	(700,±575)

3.2.4 Central Solenoid

The central solenoid is a vertical coil located in the central stack of the SMART and is responsible for inducing the plasma current throughout the experiment. It has an inner radius of 121 mm, an outer radius of 148 mm and a height of 1550 mm. It has a total of 230 turns of 11x11 mm square copper conductor.

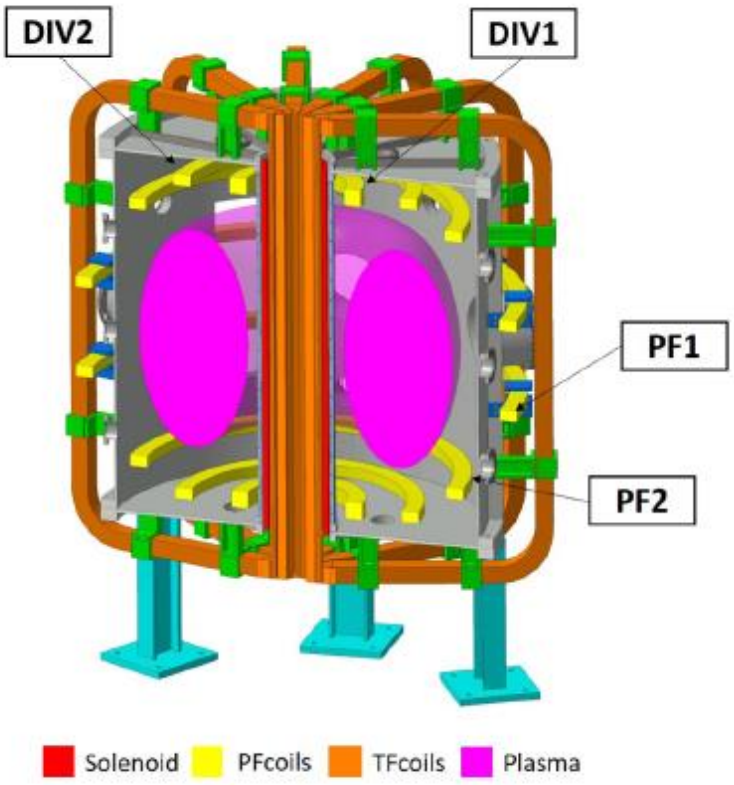

Figure 3.4. Cross Section of the SMART, reprinted from [26]

3.3 SMART Model in ANSYS

Considering the geometrical specifications of the SMART presented in the previous section, a 3D model of the different groups of coils was designed in CATIA and imported into ANSYS.

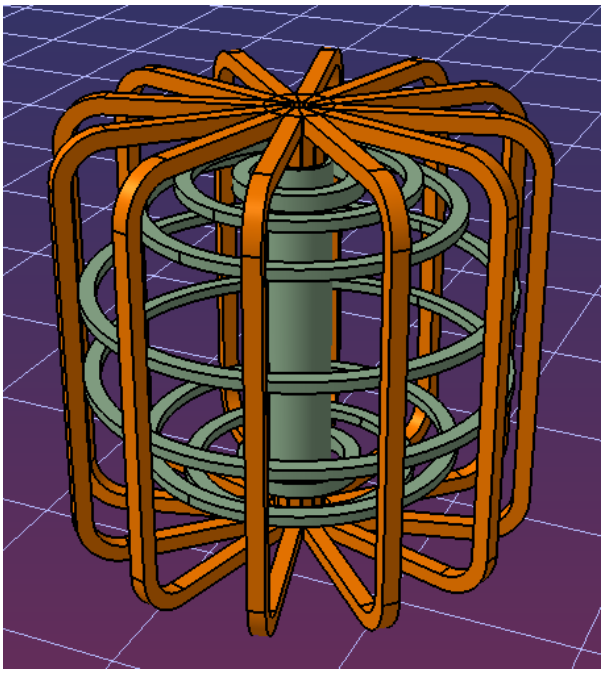

Figure 3.5 Model of the field Coils in CATIA

This model has a number of simplifications in order to optimize the simulation.

Firstly, the supports of the structure are not included in the analysis, as they are irrelevant for the measurement of the plasma current. The winding of the electromagnets has not been modelled either, as processing the geometry of the individual turns would unnecessarily complicate the generation of the Mesh. Instead, the electromagnets were taken as solid copper conductors with the same cross section, and carrying a current which is the total current ($N \cdot I$) that flows in them.

Once the 3D model of the field coils was created, the Vessel and the plasma were included to complete the ANSYS model of the SMART. For the Vessel, it has been modelled as a smooth-surfaced steel chamber with walls of the thickness specified in section 3.2.1.

In the case of the plasma, since it is not possible to recreate the properties of a real plasma, it has been modelled as a copper toroid of 50 mm radius placed in the center of the vacuum chamber, so that the current measured by the RC will be that which flows through the toroid.

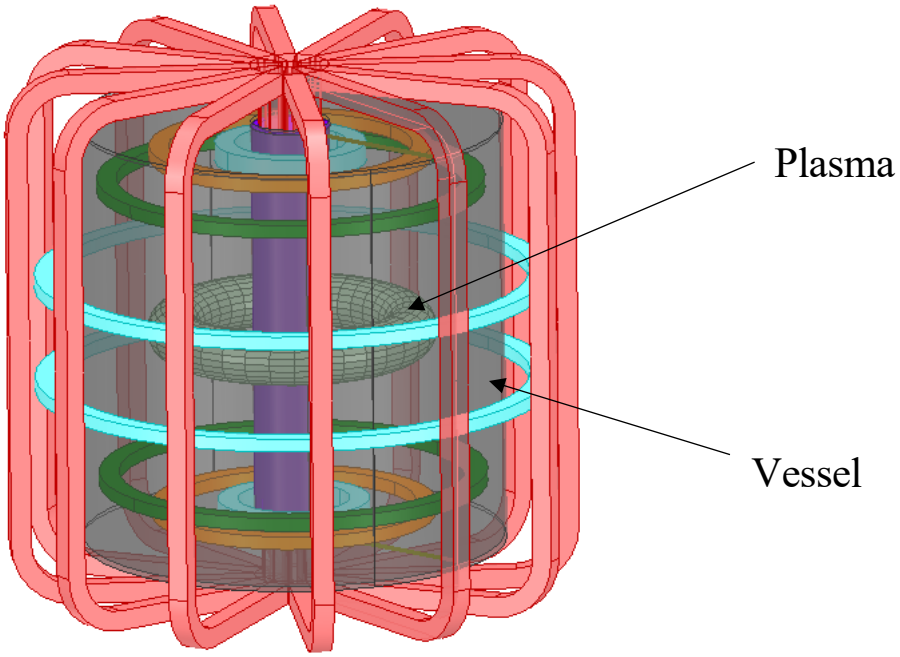

Figure 3.6 ANSYS Model of the SMART, including the Vessel and the Plasma

3.4 Rogowski Coil model in ANSYS

In order to approximate as closely as possible the behaviour of a real RC, its model has been based on a preliminary design proposed for this work, the specifications of which are detailed below:

- **Position.** As a first approach it has been chosen to place the coil in such a way that it is at all times 10 mm apart from the inside wall of the Vessel. This was estimated considering the supporting structure that will be installed for these coils. The path that the winding follows will therefore be rectangular, such as the cross-section of the chamber. Consequently, the estimated length will be 4.4 m.
- **Wire**. The wire to be used will be a copper wire with a diameter of 0.6 mm.
- **Number of turns.** The maximum number of turns that can be fitted to the RC is determined by its length and the diameter of the cable.

$$N_{max} = \frac{l}{d} \approx 7333 \text{ turns} \tag{3.1}$$

However, the machining of the coils introduces a certain pitch between turns, so the number of turns must be less than the maximum. In this case, 6700 turns have been chosen.

- **Cross-section** The core of the RC shall be of circular cross-section with a diameter of 10 mm.

Once the preliminary design parameters were known, the model was built, which was first designed in CATIA and then imported into ANSYS.

In order to be able to work efficiently with the RC model, a number of adaptations had to be made.

Firstly, the fact that the RC profile is circular adds complications when generating the Mesh, as the grid elements must adapt to the curvature, with the consequent increase in computational load. This does not happen with straight surfaces, so it was decided to approximate the circular profile of the RC to that of a regular 16-sided polygon, so that the coil is a prism rather than a cylinder. The cross-sectional area of the adapted coil becomes 97.45% of the original cross-sectional area.

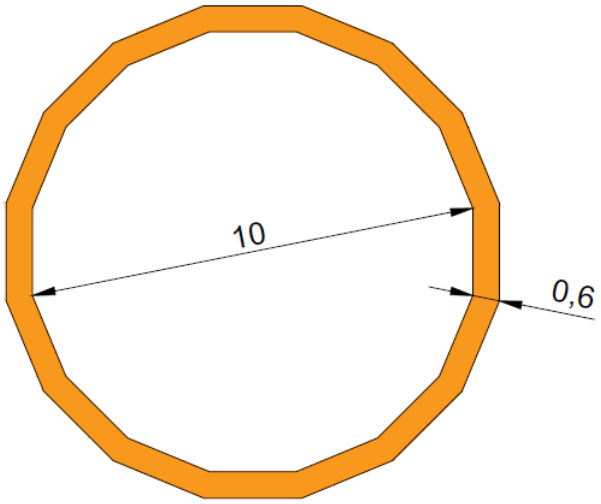

Figure 3.7 Cross-section of the adapted Rogowski Coil

As with the field coils, modelling the coil turns individually has been discarded. The coil will be modelled as a hollow copper cylinder of thickness equal to the cable diameter. The assignment of the number of turns will be done within ANSYS itself once the model has been imported.

3.5 Mesh generation

With the SMART model and the RC model imported into ANSYS, the next step to be able to simulate an experiment is to generate the Mesh.

The Mesh, as mentioned above, is the set of elements into which the model is divided for the finite element resolution. Obtaining an accurate result depends to a large extent on how this mesh has been generated. In general, the thinner the elements are, the better the quality of the simulation, but an excessive number of elements can lead to excessive simulation times. It is therefore necessary to find a balance point.

ANSYS takes care of the Mesh processing. There are two options: to use the Initial Mesh or to import it from another solution using the Adaptive Meshing tool. For the Initial Mesh, ANSYS estimates, based on the geometry of the model, how the mesh should be distributed and the size of the elements in each part. A series of parameters can be configured, such as the maximum number of elements for

a given volume or the maximum size of the elements, so that in the most critical areas of the model the mesh is more refined. However, using the Initial Mesh can give quite inaccurate results, and determining which areas need further refinement can be a very difficult task in complex models.

The second option is to import the Mesh, either manually generated or generated by ANSYS in another solution of the same model. To import it from another solution, what is usually done is to solve the same model but in magnetostatic conditions, that is, with all the electromagnetic fields constant. To solve the magnetostatic problem ANSYS uses the Adaptive Meshing tool. This is an iterative method that consists of solving the equations of the model and, depending on the error committed in the solution, adapting the Mesh, until a certain error convergence criterion is reached. Once the refined Mesh of the magnetostatic model is generated, it is imported into the transient model for the simulation.

For the SMART model, the second option has been chosen, choosing as convergence criterion a maximum error of 0.5 %.

The most important characteristics of the generated Mesh are shown in the following table.

Table 3.2 Statistics of the generated Mesh, extracted from ANSYS

	RC	**Plasma**	**PF1**	**PF2**	**DIV1**	**DIV2**	**Vessel**
Number of elements	11504	7829	247	177	170	157	9469
Minimum Edge length [mm]	2.21	27.59	91.86	102.88	86.24	90.14	6.39
Maximum Edge length [mm]	97.42	136.149	260.03	310.37	166.19	194.77	322.32
Mean Edge legth [mm]	41.04	67.83	171.238	172.77	115.15	145.47	131.27

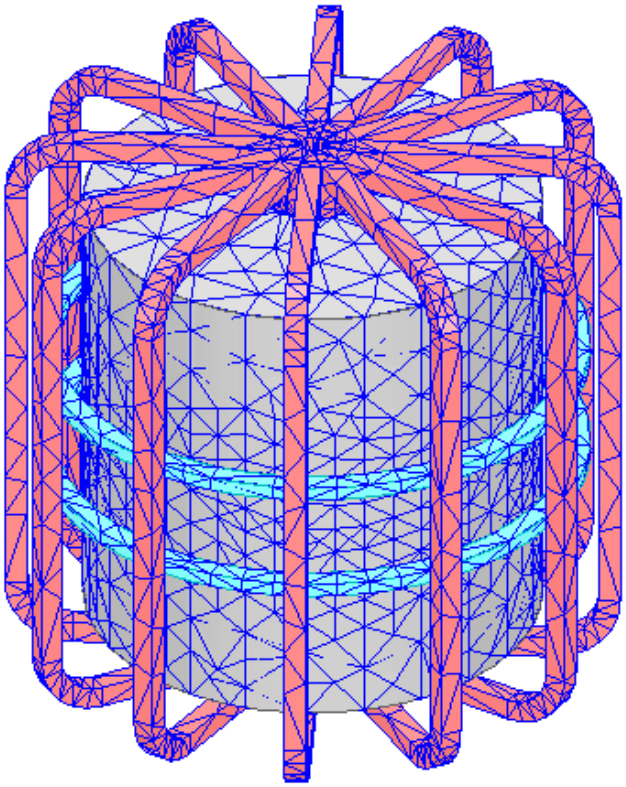

Figure 3.8 External view of the model Mesh

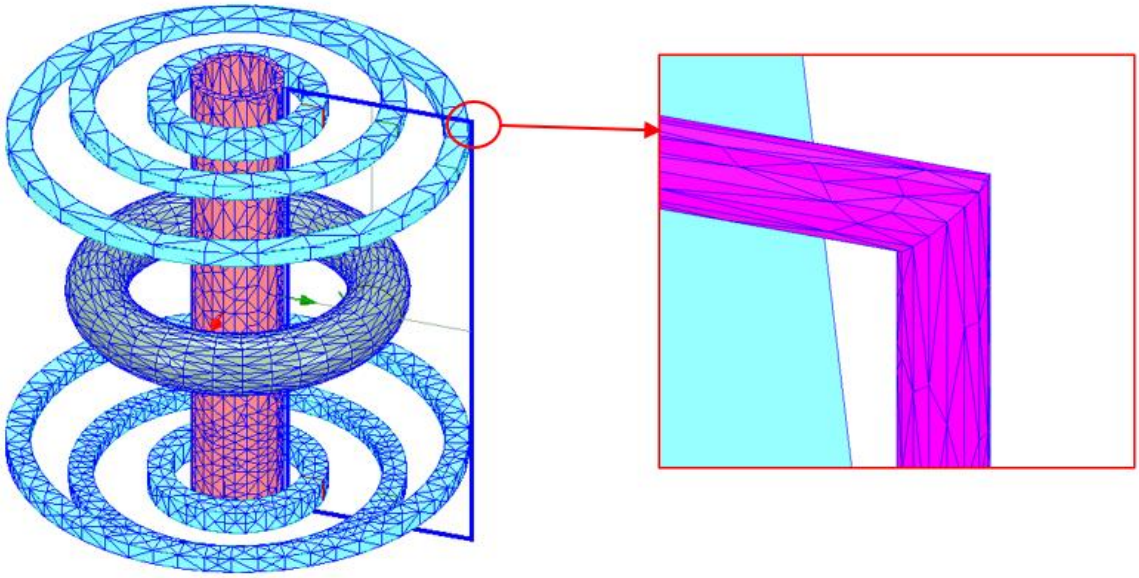

Figure 3.9 Internal view of the model Mesh

4 RESULTS OF THE SIMULATIONS

This chapter will describe how the data were collected and processed and will present the results obtained in comparison with the corresponding reference values.

4.1 Procedure for obtaining the results

The procedure to obtain the results comprises two parts: a first part developed in ANSYS, in which, by simulating the model described in section 3, the values of the induced voltage in the RC are obtained; and a second part in Matlab, where, from the values obtained in ANSYS, the evolution of the plasma current is reconstructed, to finally compare it with the reference values.

Figure 4.1 Flow chart of the procedure used to obtain the results

ANSYS Simulation

The ANSYS model of the SMART described in chapter 3 is used to simulate the voltage that would be induced during the SMART operation in a RC with the characteristics described in Chapter 3. In this case, phase 2 of the device has been chosen as the basis for the simulations, although data from other phases of the SMART will be also used.

As mentioned above, the SMART electromagnets are divided into 6 independent groups: TFC, PF1, PF2, DIV1, DIV2, and the central solenoid. Each of these groups is passed a current to generate the appropriate magnetic field inside the Tokamak, so that it can hold the plasma inside it under the required conditions.

For this simulation, both the currents flowing through the 4 pairs of poloidal field coils and the plasma current are known. Their curves, shown in figures 4.1 and 4.2, have been provided by the PSFT Group, obtained by solving the plasma dynamic and equilibrium equations for the conditions specified for phase 2 (100 kA for 100 ms).

The TFC current has not been taken into account, assuming that the effect of the toroidal magnetic field on the induced voltage in the RC will be cancelled in reality with a return loop, as explained in section 2.2.

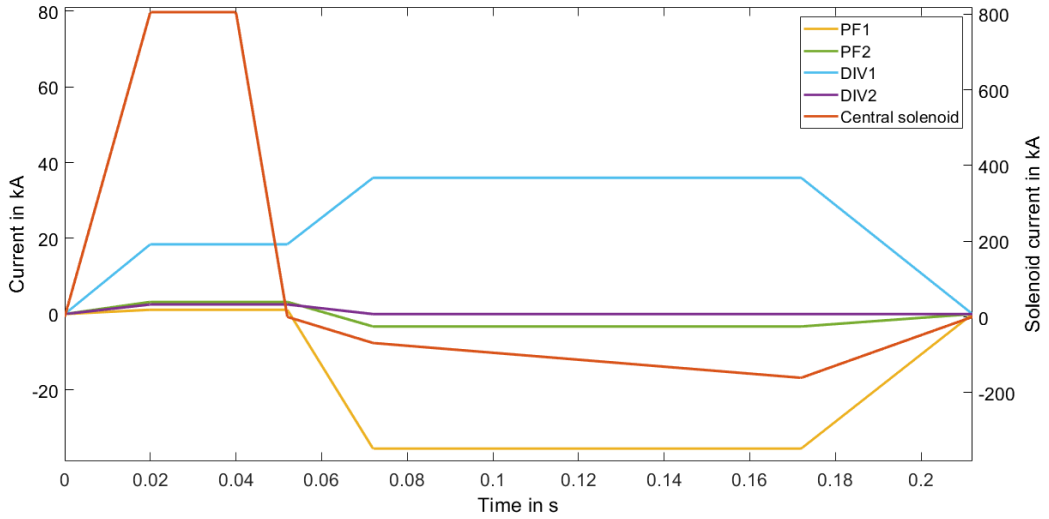

Figure 4.2 PFC and Central Solenoid current profiles

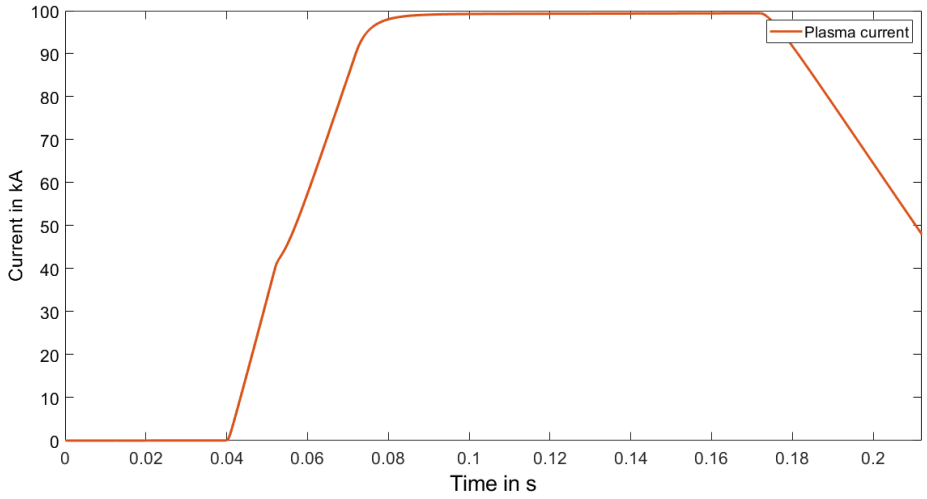

Figure 4.3 Plasma current profile

To incorporate these values into the ANSYS model, the procedure is as follows: the cross-section of the 3D model of the corresponding coil is taken, the number of turns is defined and a current curve is assigned, so that the assigned current corresponds to the current flowing through each of these turns. In the case of PFC and plasma, as they are considered to be solid copper conductors that carry the total current ($N \cdot I$), they have been assigned a single turn.

As for the RC, it has been assigned a zero current and a number of conductors, i.e. turns, of 6700, so that the voltage calculated by ANSYS corresponds to the open-circuit voltage between the terminals of the coil.

With the model prepared, the simulation was run with a step of 1 ms, finally obtaining the evolution of the induced voltage.

MATLAB Postprocessing and comparison

The following code programmed in Matlab has been used for the calculation of the plasma current.

```
function [M,R,L,V_rog,V_rog_teorica,I_plasma,I_plasma_ref,time1,time2]
=curvas(I_plasma_tab,V_ansys,num_vueltas)
% Rogowski coil data
l=4.4;          % Length
d=0.0006;       % Wire diameter
D=0.01;         % Cross-section diameter
mhu=4*pi*1e-7;  % Magnetic permeability
A=(pi*D^2)/4;   % Cross-section Area
A_pol=A*0.9745; % Corrected cross-section area
a=pi*(d^2)/4;   % Wire cross-section area

% Mutual inductance
M=mhu*num_vueltas*A/l;

% Input plasma current values
delimiter=' ';
Perfil_plasma=tdfread(I_plasma_tab,delimiter);
r=fieldnames(Perfil_plasma);
if strcmp(r{1},'x0_0')==1
    I_plasma_ref=Perfil_plasma.x0_0(:,2);
    time1=Perfil_plasma.x0_0(:,1);
else
    I_plasma_ref=Perfil_plasma.x01;
    time1=Perfil_plasma.x0;
end


if isempty(strfind(Rog_ansys.textdata{5},'mV'))==0
    V_rog=Rog_ansys.data(:,2)*1e-3;
end


% Imported induced voltaje from ANSYS
delimiter=' ';
headerlines=7;
Rog_ansys=importdata(V_ansys,delimiter,headerlines);
if isempty(strfind(Rog_ansys.textdata{5},'mV'))==1
    V_rog=Rog_ansys.data(:,2);
end
time2=Rog_ansys.data(:,1)/1000;

% Reconstruction of the plasma current

I_plasma=cumtrapz(time2,V_rog)/(M);
```

First of all, the geometrical parameters of the RC are defined, which are necessary for the calculation of the mutual inductance.

The mutual inductance calculated in Matlab is $1.5029 \cdot 10^{-7}\ \frac{\mathrm{V \cdot s}}{\mathrm{A}}$.

Once the mutual inductance has been calculated, the values of the induced voltage in the RC imported from ANSYS are extracted. The curve defined by these values is integrated with respect to time and divided by the mutual inductance, thus obtaining the evolution of the plasma current.

4.2 Results

4.2.1 First tests

To check that the model is able to reconstruct the plasma current with sufficient accuracy, a series of tests were performed in which all field coils were switched off and only the plasma was left on, so that the only current flowing within the area enclosed by the RC was that of the plasma.

First, the plasma was assigned a simplified current profile, consisting of a ramp-up from 40 ms to 100 ms of 1666.67 A/s, until 100 kA were reached.

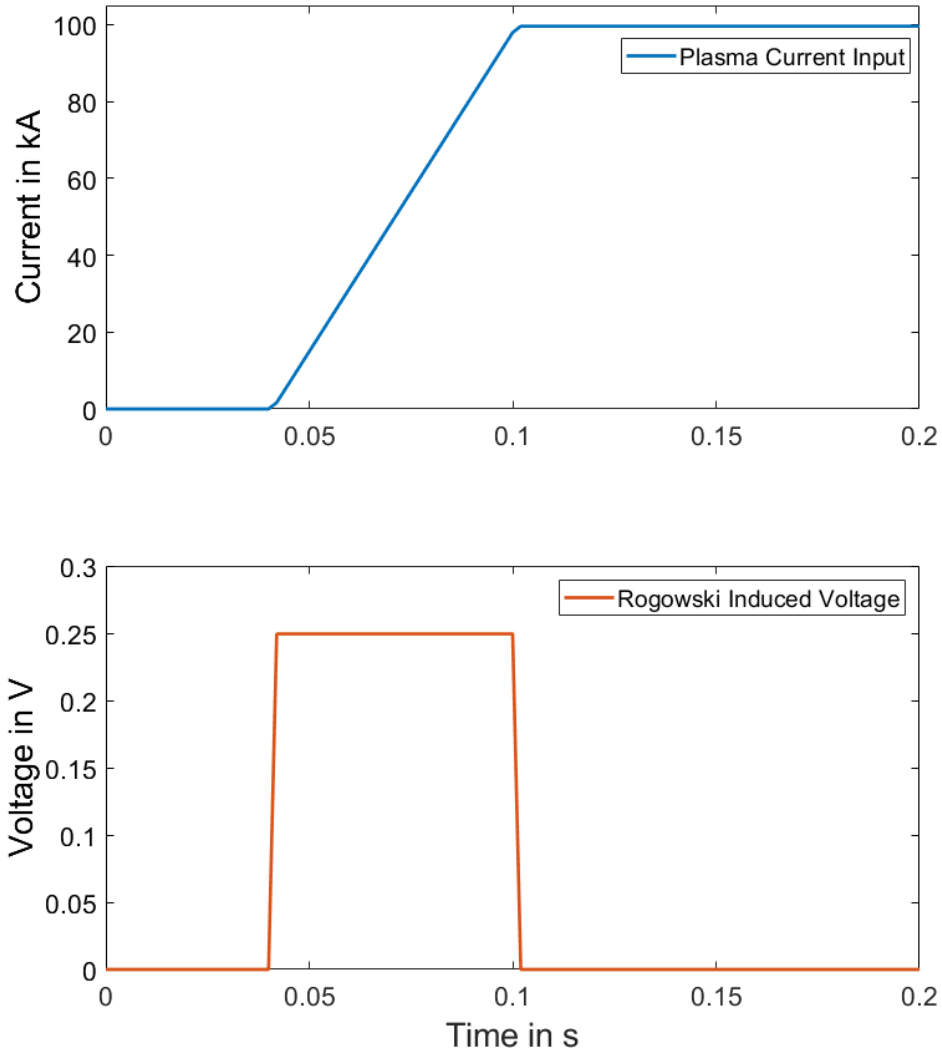

Figure 4.4 Simplified plasma current and corresponding induced voltage in the Rogowski coil

A square voltage is induced in the RC when the current starts to rise, because the derivative of the ramp is constant during the ascent and zero the rest of the time.

The maximum voltage reached is 249.5 mV.

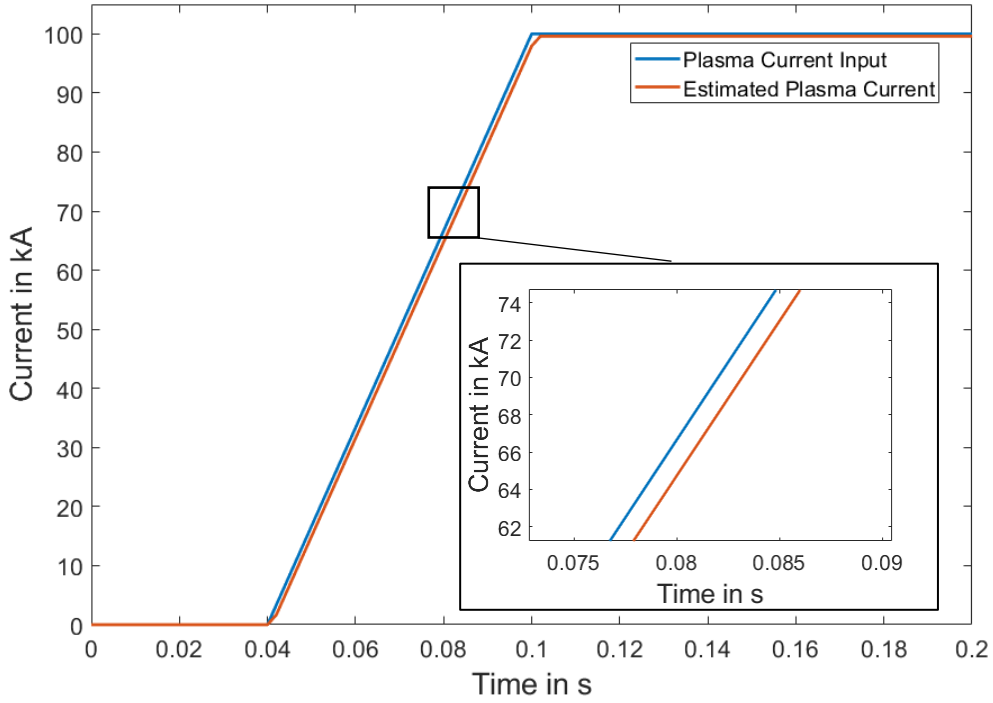

Figure 4.5 Estimated plasma current compared to reference

As can be seen in the figure, the reconstructed current is close to the reference, although a slight delay is observed in the curve, which may be caused by the error introduced by the 1 ms step. The error during the flattop is 0.4 %.

Once it was found that good results were obtained with a simplified curve, the current values provided by the PSFT Group for phase 2 were assigned to the plasma.

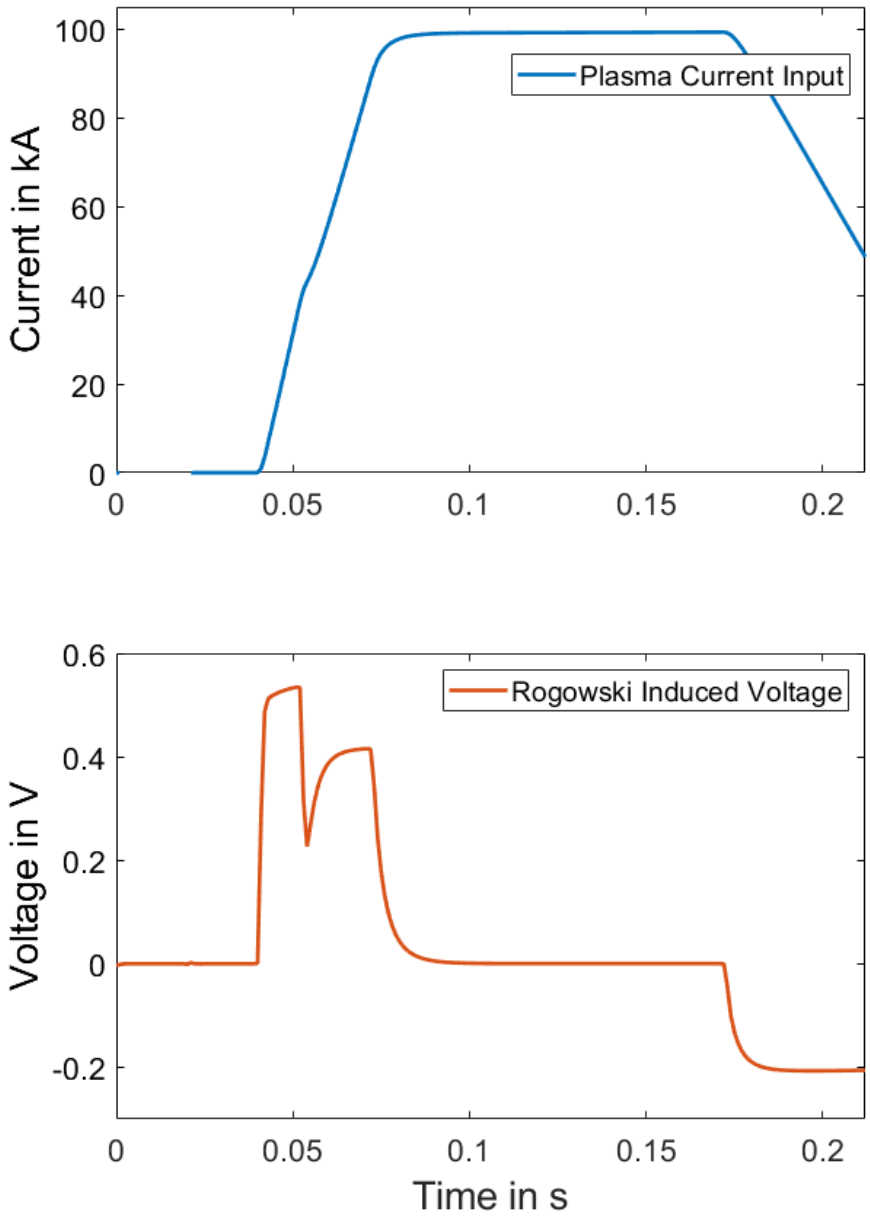

Figure 4.6 Phase 2 plasma current and corresponding induced voltaje in the Rogowski coil

In this case, the maximum RC voltage exceeds 500 mV, since the slope of the current is bigger in this case.

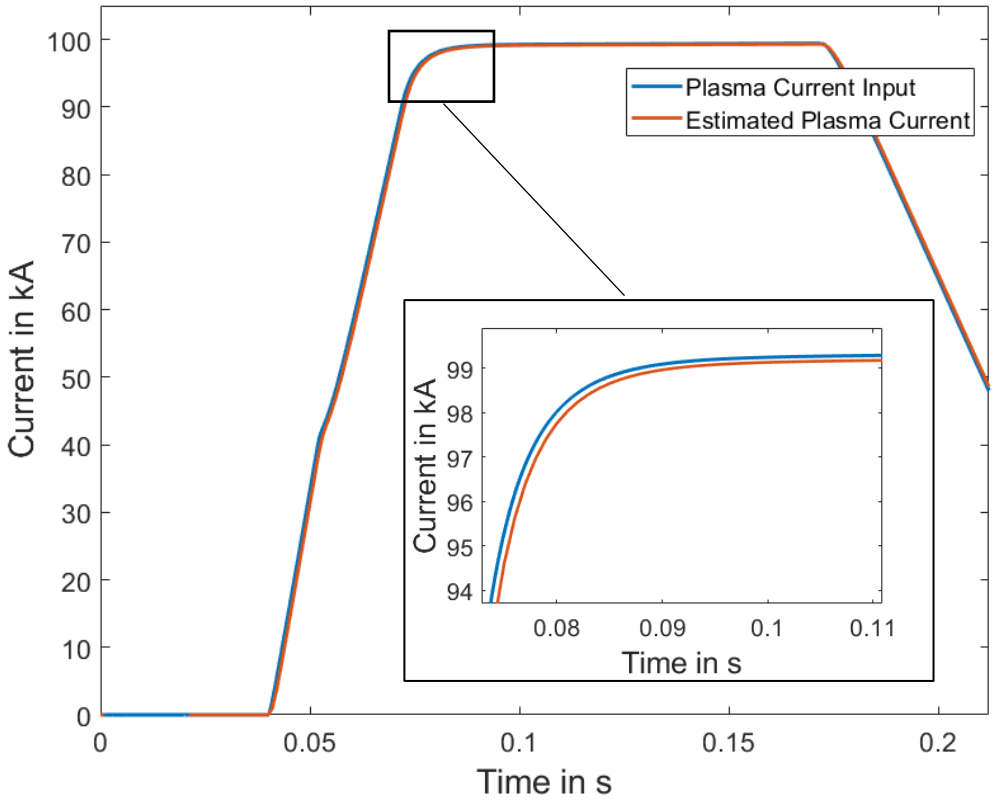

Figure 4.7 Estimated plasma current compared to reference

Again, the RC is able to detect quite accurately the evolution of the plasma current, whether the trend changes sharply or more smoothly. The flattop error remains at 0.11 %.

To check whether the RC responds correctly to a wide range of current values, tests were made with other current profiles provided by the PSFT Group for phases 1, 2 and 3, reaching 30 kA, 200 kA and 400 kA respectively.

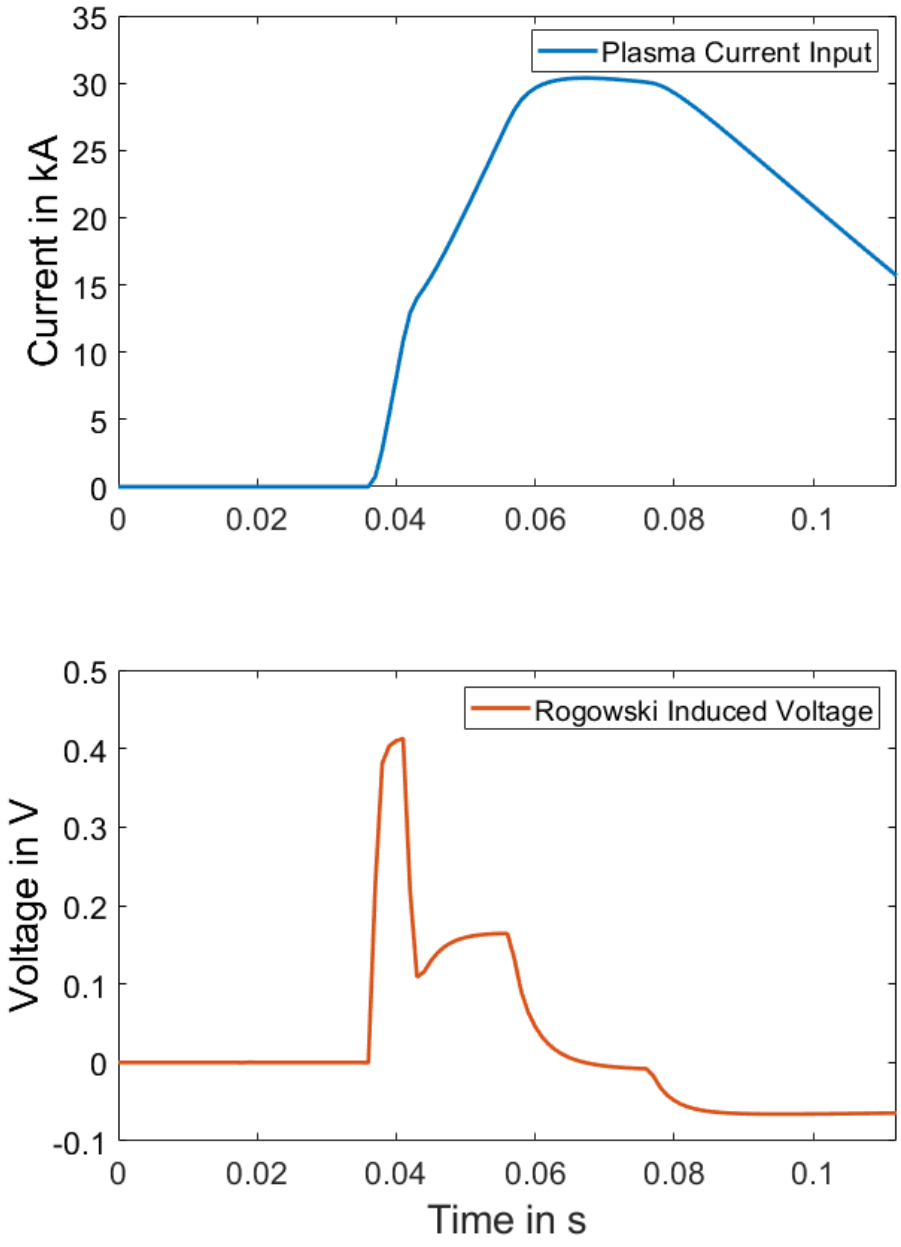

Figure 4.8 Phase 1 plasma current and corresponding induced voltage in the RC

The maximum voltage reached is 430 mV.

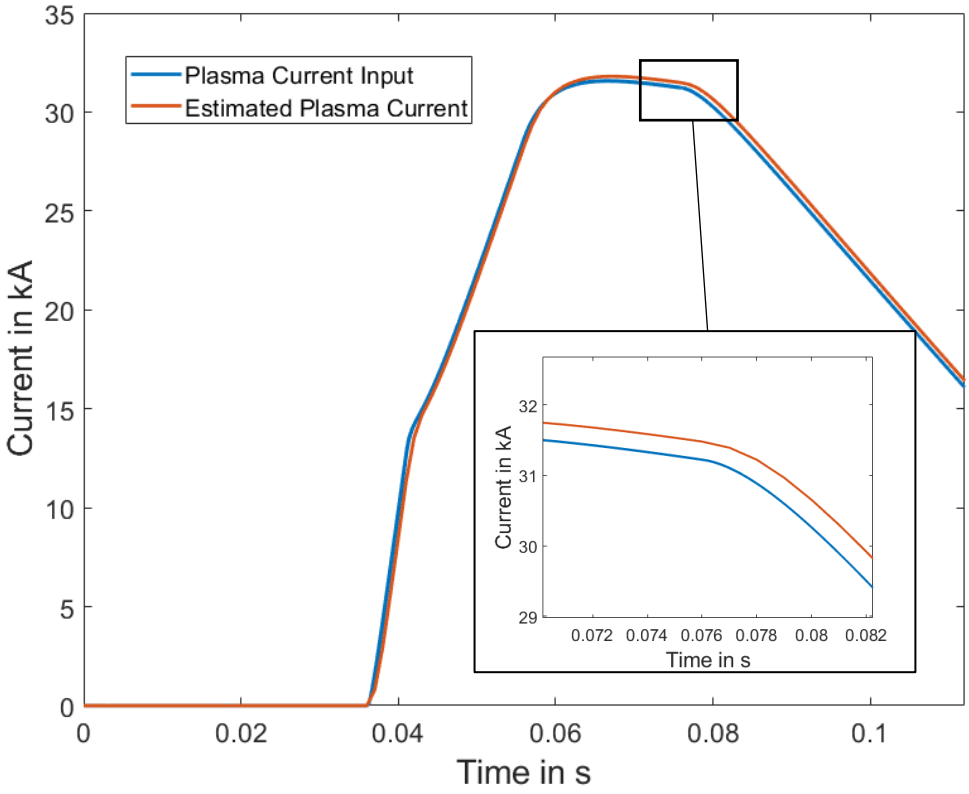

Figure 4.9 Estimated plasma current compared to reference

During the flat-top an error of 0.6 % is shown.

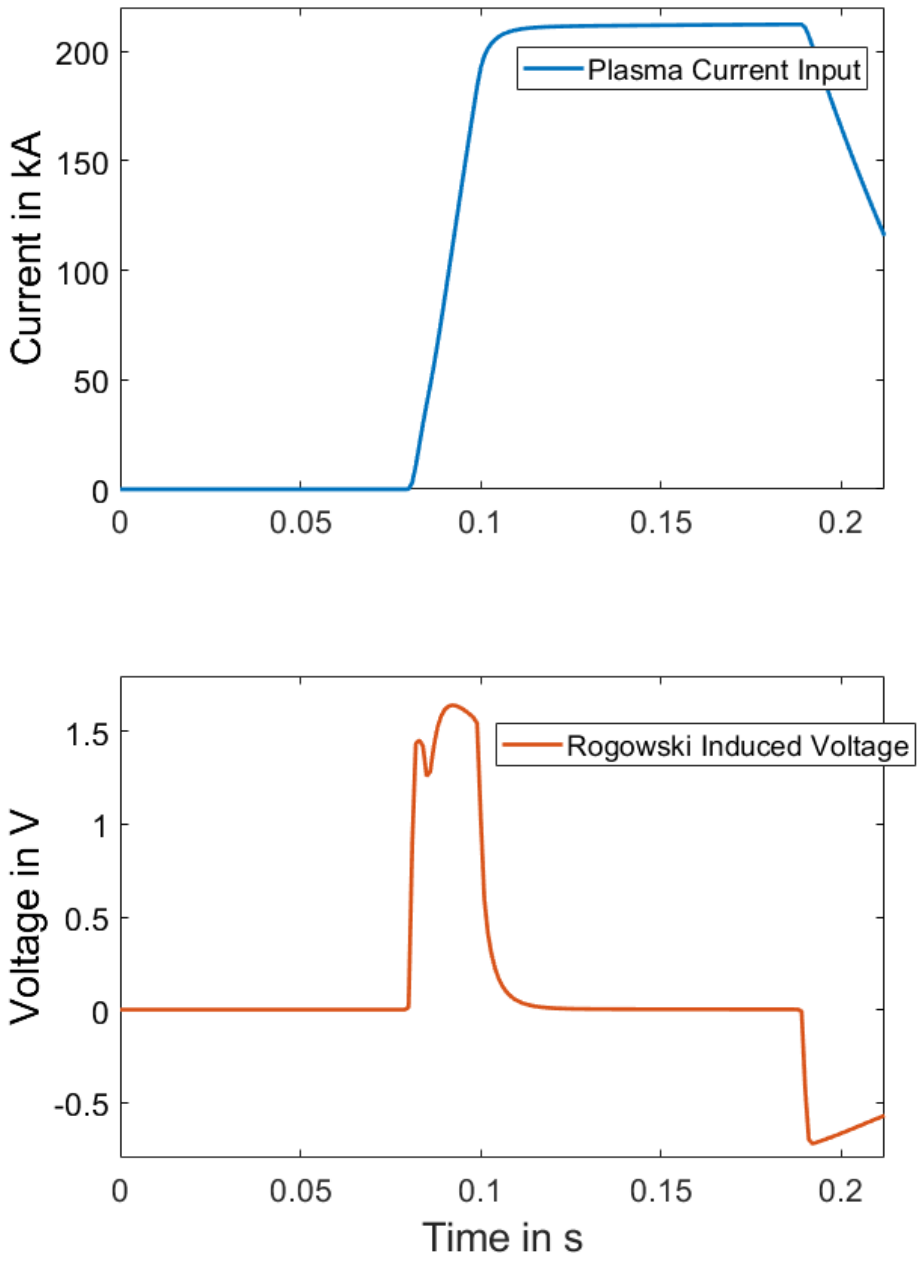

Figure 4.10 Phase 2 200 kA plasma current and corresponding induced voltage in the RC

In this case, the maximum voltage reached is 1.64 V.

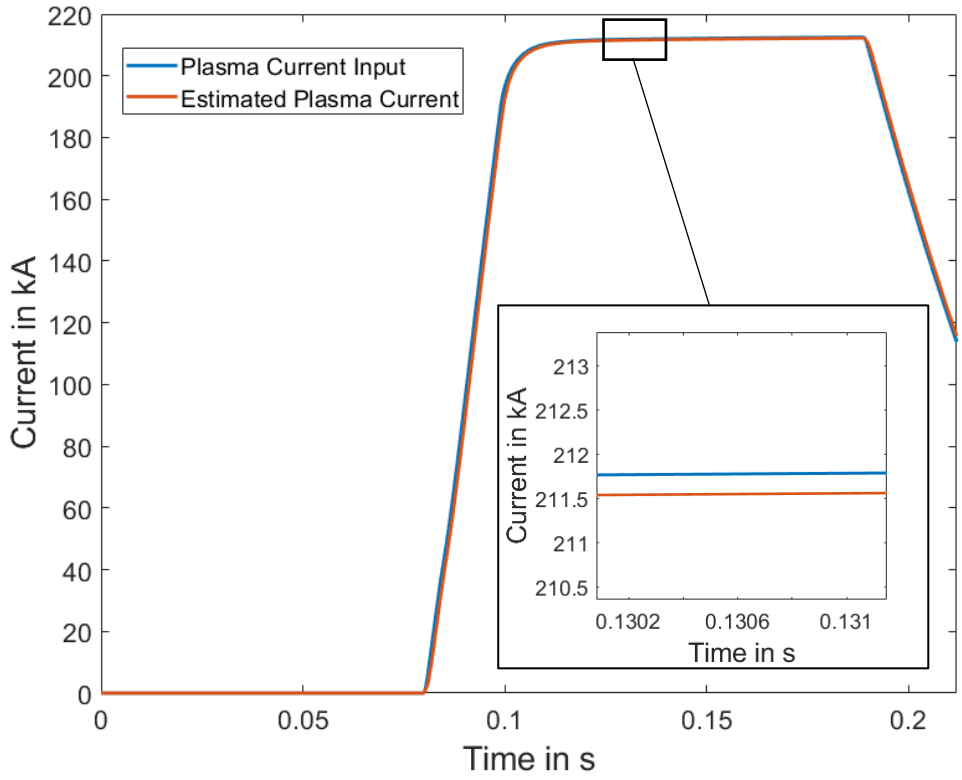

Figure 4.11 Estimated plasma current compared to reference

The error with respect to the reference during the flat-top is 0.1 %.

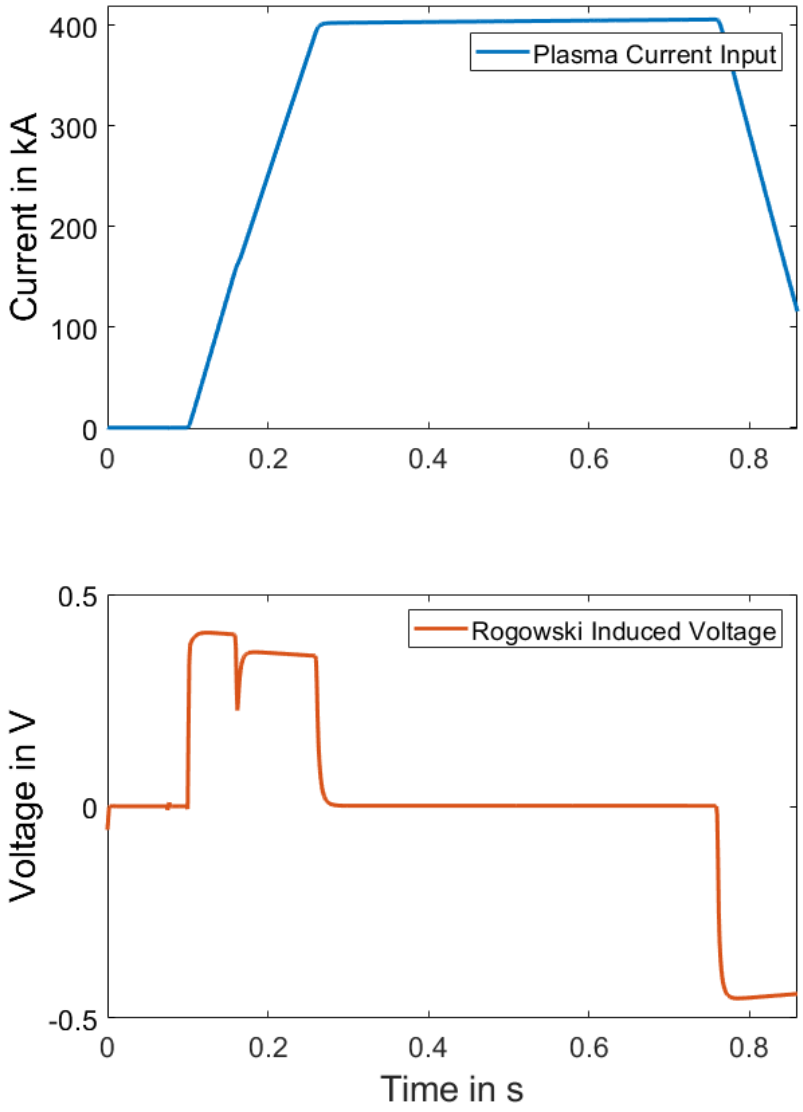

Figure 4.12 Phase 3 400 kA plasma current and corresponding induced voltage in the RC

In this case, the highest voltage in absolute terms occurs towards the end of the simulation, with a negative peak voltage of 450 mV.

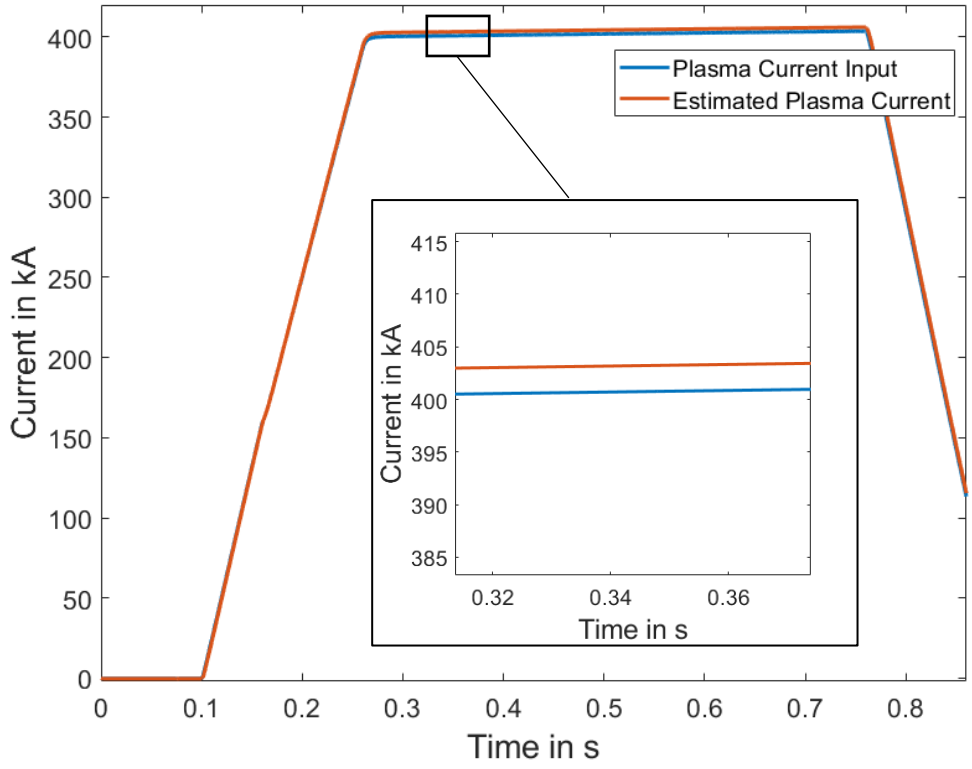

Figure 4.13 Estimated plasma current compared to reference

The error in this case stays at 0.6 % during the flat-top.

Based on the results of the first tests, it is safe to say that the model works well and that the RC is able to perceive and reconstruct a wide range of plasma currents.

4.2.2 Influence of the PFC

Ideally, the current recreated from the voltage induced in a RC is equal to the total current passing through the area it encloses.

In this case, as placed in the model, not only does the plasma current flow through this area, but also the currents of the poloidal field coils inside the vacuum chamber, i.e., DIV1, DIV2 and PF2.

Therefore, these coils will also induce a voltage in the RC, so that the current reconstructed from this voltage should correspond to the sum of their currents and that of the plasma. The central solenoid and PF1 are outside the Rogowski coil domain, so they should not influence the current measurement.

To filter the plasma current measurement, it will be necessary to subtract the contributions from the rest of the coils.

$$I_{plasma} = I_{total} - I_{PF2} - I_{DIV1} - I_{DIV2} \tag{4.1}$$

To corroborate this and prove that the plasma current can be easily filtered out when operating with the real RC, the model was simulated by activating both the plasma and the SMART coils.

The obtained voltage has been integrated as before in Matlab to obtain the total current, and in the end the known currents of the PF2, DIV1, DIV2 coils, shown in section 4.1, have been subtracted. Finally, the resulting current has been compared with the reference.

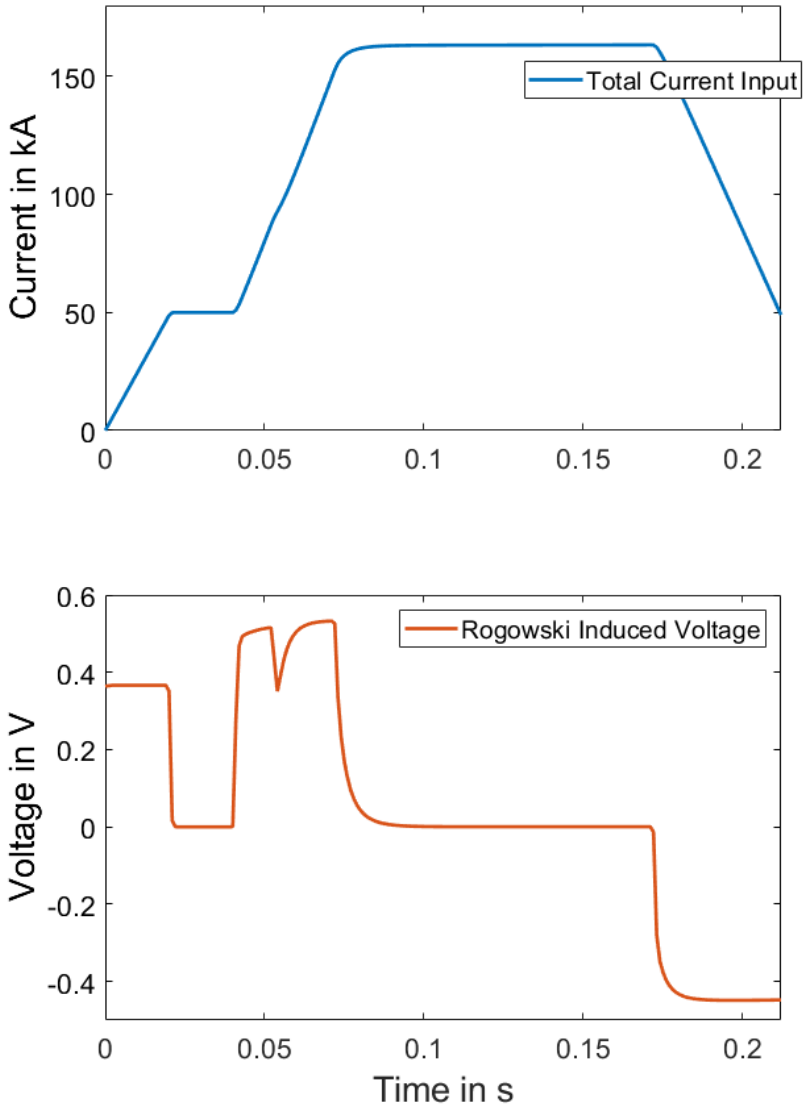

Figure 4.14 Total current inside the Vessel and corresponding induced voltage in the RC

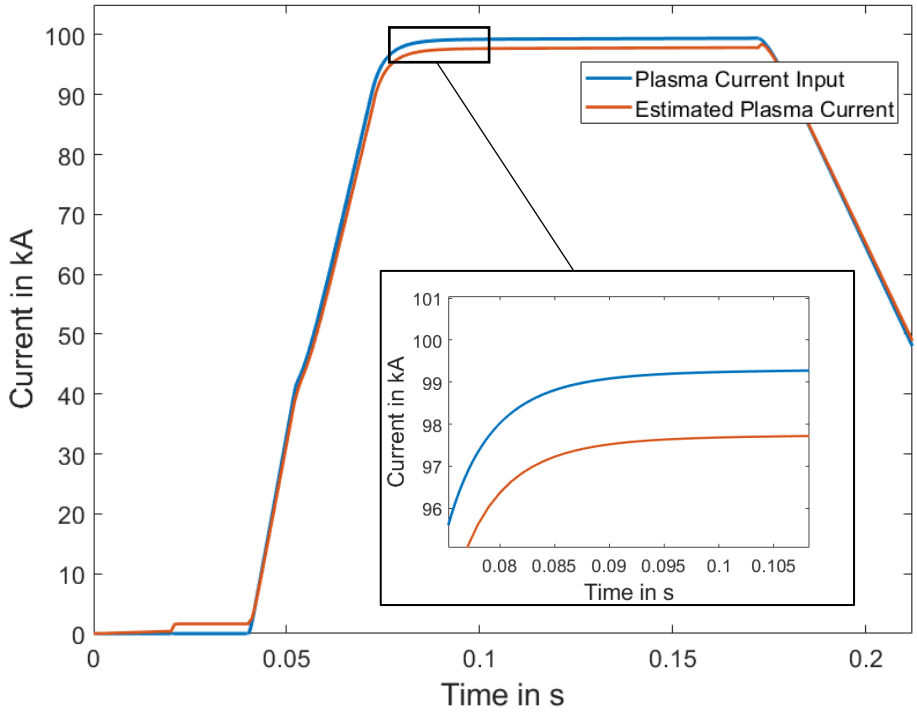

Figure 4.15 Estimated plasma current compared to reference

Although there is a slight increase in the error, which rises to 1.6 % at the flat-top, the reconstruction still reflects the evolution of the plasma current fairly closely.

4.2.3 Plasma events

Plasma in a Tokamak can be affected by instabilities that can cause sudden movements inside the vacuum chamber (so called Virtual Displacements Events) or sudden cooling that causes the plasma current to drop suddenly (so called Disruptions). The capability of the RC to detect these short-lived events will be crucial for the correct diagnosis of the plasma.

It is therefore interesting to study how the RC behaves in such scenarios. With the help of the ANSYS model, plasma shutdown and movement scenarios have been recreated.

Plasma Disruption

To simulate a plasma disruption, an absolute current drop of 4 ms duration was assumed. This duration was chosen by estimating the time constant of the plasma [27]. The curve corresponding to phase 2 was taken and, at 104 ms, once the nominal value of 100 kA was reached, a ramp down was imposed until the current was completely cancelled, so that at 108 ms the plasma current was 0.

The results of the induced voltage and reconstructed current are shown below.

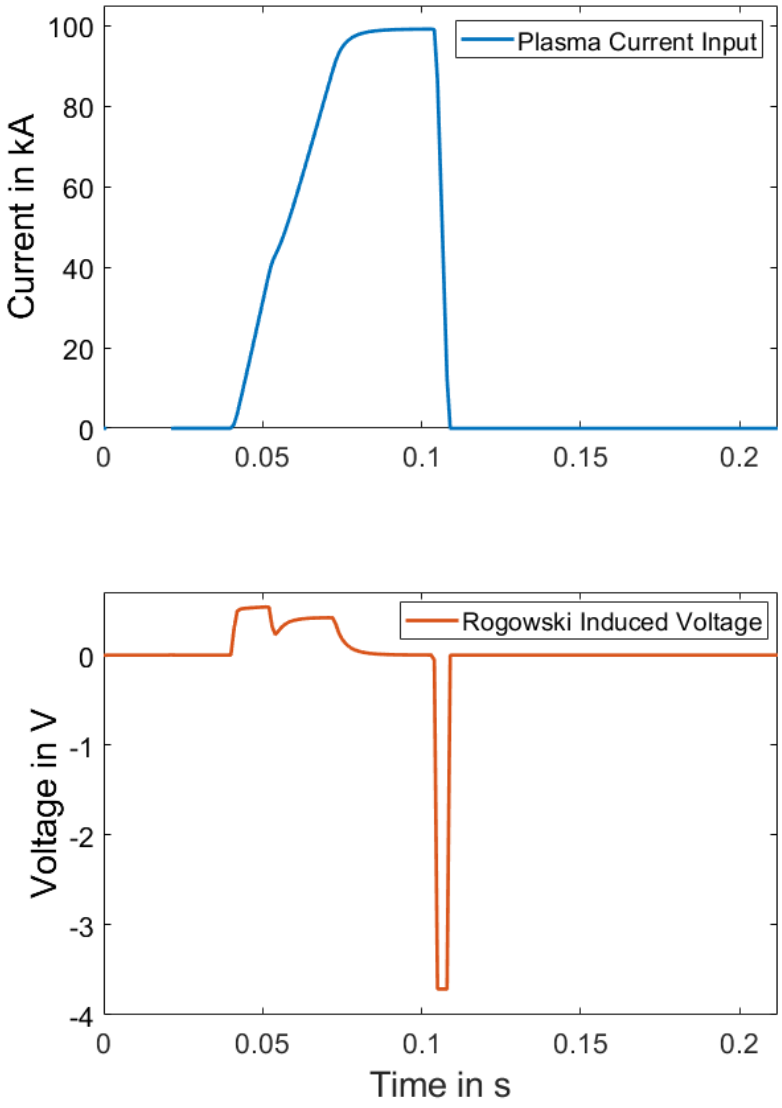

Figure 4.16 Plasma turned off at 104 ms and corresponding induced voltage in the RC

As can be seen in figure 4.16, when the plasma current is turned off, a negative voltage peak of -3.7 V is produced, which is much more prominent than the one caused during the plasma start-up.

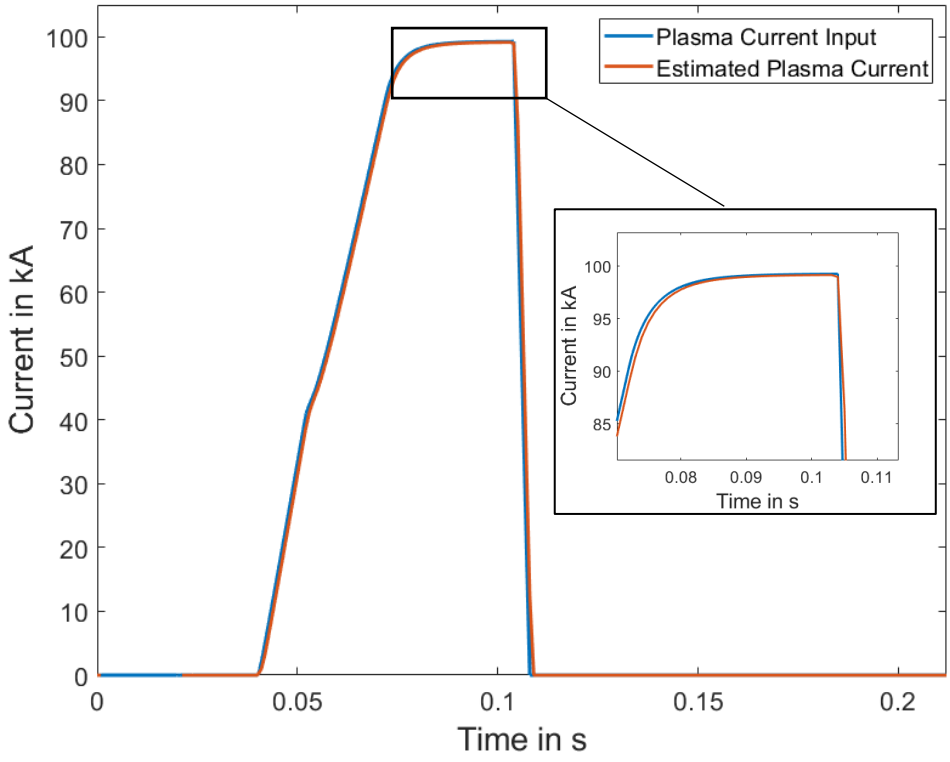

Figure 4.17 Estimated plasma current compared to reference

The reconstruction of the current is very well approximated even during sudden switch-off, with virtually no delay.

Plasma Vertical Displacement Events

Keeping the plasma in a specific position in the vacuum chamber requires a very precise control of the magnetic field. During the experiments it is possible that significant deviations in position can occur.

The RC measures the current flowing through the area it encloses. If the plasma changes position but its current remains the same, the RC measurement should not be affected, since the amount of current flowing through its area does not change.

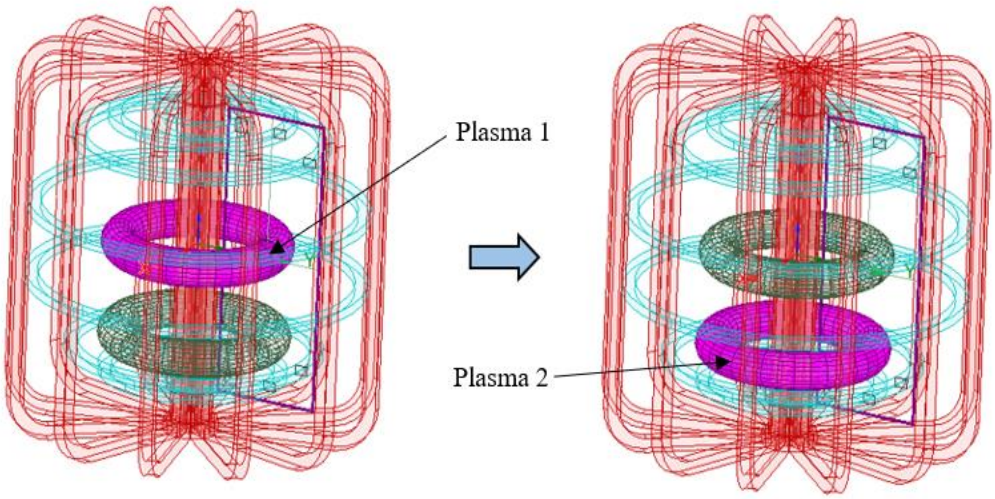

Figure 4.18 ANSYS Models of the original and the relocated plasma toroid

To test this hypothesis, such an event was recreated in ANSYS. For this purpose, a second copper toroid identical to the one modelled for the plasma, but placed 450 mm below it, was modelled (Figure 4.18). The recreation will consist of, for a given moment, switching off the current flowing through the model of the original plasma and at the same time switching on the transferred plasma, so that the whole is equivalent to the plasma having moved. Subsequently, the current of the transferred plasma shall also be switched off.

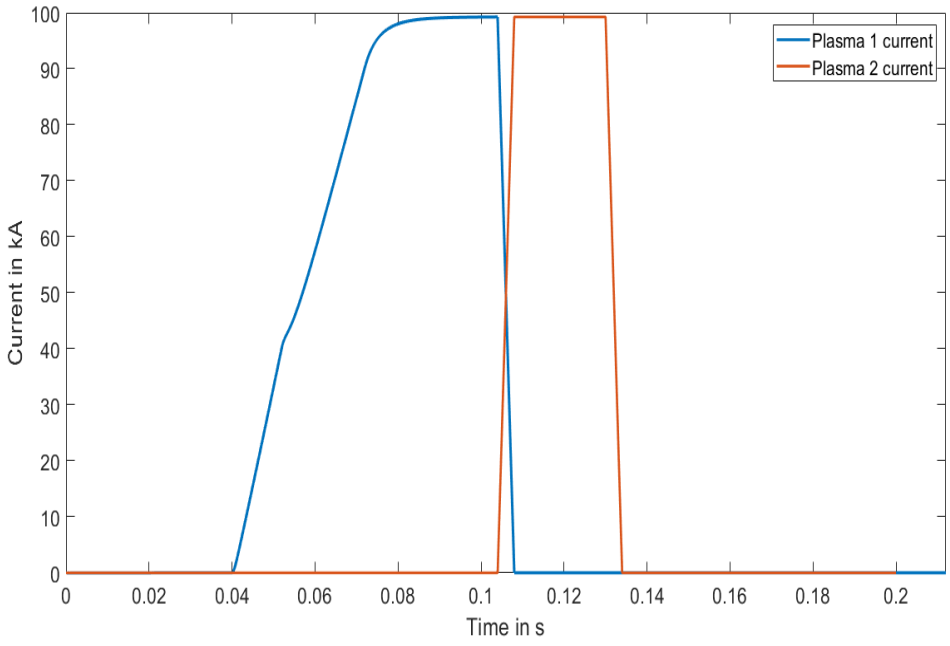

Figure 4.19 Input currents for the simulation of the movement of the plasma

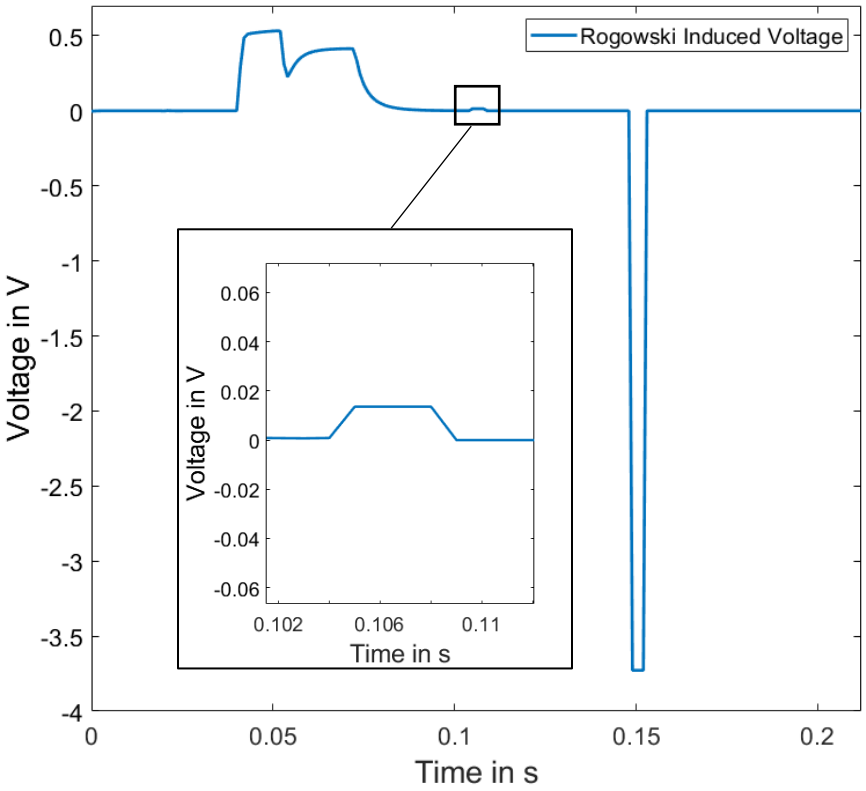

Figure 4.20 Induced voltage in the RC during the plasma movement simulation

As can be seen from the graphs, the RC is not sensitive to the movement of the plasma inside the vacuum chamber, as the total current inside the RC does not change. Only a slight increase in voltage is observed between 104 and 108 ms, but it is practically negligible.

5 CONCLUSIONS AND FUTURE WORK

5.1 Conclusions

The main objective of this work, which is to contribute to the design of a plasma current measurement system for the SMART, has been successfully fulfilled.

To this end, the use of RCs has been suggested. After introducing the theoretical concepts on which the operation of RCs is based, a preliminary design of the coil, based on the geometrical characteristics of the SMART, has been proposed. It has been then transferred to a 3D model and integrated with the 3D model of the SMART, placing it inside the vacuum chamber. A number of simulations have been carried out, recreating the behaviour of the plasma and the field coils in different scenarios. In this way, it has been possible to estimate the response of the coil during the operation of the SMART and to check its efficiency as a sensor of the plasma current.

In view of the results of the simulations, it can be concluded that implementing RCs for this application is a suitable option. The coil has been shown to be very reliable in detecting plasma currents of very different shape and magnitude. Moreover, the response to irregular plasma behaviour is fast and accurate, which makes the RC very attractive for a correct diagnosis of the causes of plasma instabilities. However, it lacks on perceiving the movement of the plasma.

Additionally, using the same methodology, work was done on an external RC model that could detect the induced current in the vacuum vessel. However, due to the added complications it introduced in the simulation, it was decided to be excluded of the work, leaving it as a task to be developed in the future.

5.2 Future work

This work has served as a first step towards the implementation of a control system that will allow to track the evolution of the plasma and to act on it in real time. To continue in this line of work, the following tasks are proposed:

- Design of the integrator circuit

In order to infer the evolution of the plasma current during the experiments, an integrator circuit must be added to the coil. The design will require, among other tasks, choosing the most suitable circuit topology and performing a frequency analysis in order to choose the electrical parameters that will satisfy the correct operation of it.

- Integration with the power supply

Plasma monitoring would allow instabilities to be identified and corrected by modifying the current of the SMART field coils accordingly. It would therefore be interesting to integrate the Rogowski coil signal into the control of the power supplies so that, if anomalies are detected in the plasma, it would be possible to act on it directly and restore stability.

- Measuring the Vessel's Eddy Currents

In addition to the plasma current, the current induced in the SMART Vessel should also be measured. The Vessel is made of steel, so in the presence of strong variations of the magnetic fields produced by the field coils and the plasma, large currents will be induced, which will have to be considered when calculating the electromechanical stresses that the chamber has to withstand. It is proposed to design an external Rogowski coil around the Vessel in order to detect these eddy currents.

- Plasma motion detection

As explained above, the Rogowski coil is not sensitive to changes in plasma position. A task to be developed would be to include another detection system capable of sensing this movement, such as Mirnov coils, so that, together with the Rogowski coil, an idea of both the position and the magnitude of the plasma current can be obtained during the experiments.

6 REFERENCES

[1] *Potencia instalada | Sistema Eléctrico Nacional.* (2022, July). Red Eléctrica Española. https://www.ree.es/es/datos/generacion/potencia-instalada

[2] Gómez Expósito, A., & Abur, A. (2002). *Análisis y operación de sistemas de energía eléctrica*. Madrid: McGraw-Hill Interamericana de España, pp. 217-260.

[3] McCracken, G. M., Stott, P. E., & Stott, P. E. (Peter E.) . (2005). *Fusion the energy of the universe*. Burlington, MA: Elsevier Academic Press.

[4] *Binding Energy Curve* (n.d.). Splung. http://www.splung.com/content/sid/5/page/benergy

[5] Kikuchi,M., Lackner, K. & Tran, M. Q. (2012) *Fusion physics*. Vienna: International Atomic Energy Agency.

[6] Miyamoto, K. (2016). *Plasma Physics for Controlled Fusion* (2nd ed. 2016.). https://doi.org/10.1007/978-3-662-49781-4

[7] Zohm, H. (2015). *Magnetohydrodynamic stability of tokamaks* (pp.15-37). Weinheim, Germany: Wiley-VCH Verlag GmbH & Company KGaA.

[8] Stacey, Weston M. (1984). *Fusion : an introduction to the physics and technology of magnetic confinement fusion* (pp. 1-59). New York: Wiley. http://www.loc.gov/catdir/toc/onix01/83021713.htm

[9] *Self-sustained D-T fusion reactions and triple-product criterion for ignited plasma in magnetic confinement devices* (n.d.). https://ebrary.net/174595/mathematics/sustained_fusion_reactions_triple_product_criterion_ignited_plasma_magnetic_confinement_devices

[10] *Stellerator* (2022, April 2). Wikipedia. https://en.wikipedia.org/wiki/Stellarator

[11] Samimi, Mohammad Hamed & Mahari, Arash & Farahnakian, Mohammad & Mohseni, H.. (2014). *The Rogowski Coil Principles and Applications: A Review.* IEEE Sensors Journal. 15(2), 651-658. https://doi.org/10.1109/JSEN.2014.2362940.

[12] Wang, Kangping & Yang, xu & Li, Hongchang & Wang, Laili & Jain, Praveen. (2017). *A High-Bandwidth Integrated Current Measurement for Detecting Switching Current of Fast GaN Devices.* IEEE Transactions on Power Electronics. 33(7), pp. 6199-6210. https://doi.org/10.1109/TPEL.2017.2749249.

[13] *RC Integrator | Theory* (n.d.). http://www.evalidate.in/lab1/pages/RC/RCIntegrator/RCIntegrator_T.html

[14] W. Stygar & G. Gerdin, (1982) *High Frequency Rogowski Coil Response Characteristics.* IEEE Transactions on Plasma Science. 10 (1), pp. 40-44. https://doi.org/10.1109/TPS.1982.4316132

[15] *IEEE Guide for the Application of Current Transformers Used for Protective Relaying Purposes.*(2008) IEEE Std C37.110-2007 (Revision of Std C37.110-1996). pp. 1-90. https://doi.org/10.1109/IEEESTD.2008.4483716.

[16] Balshaw, N.H. (2012, April). *Comparison Table of 'Conventional' Tokamaks.* http://golem.fjfi.cvut.cz/wiki/History/table-of-tokamaks.pdf.

[17] Eydan, Anna, Shirani, Babak, Asgarian, Mohammad Ali, Sadeghi, Yahya, & Noori, Ehsanollah (2020). *Design and fabrication of an optimized Rogowski coil for plasma current sensing and the operation confidence of Alvand tokamak. Nuclear Engineering and Technology*, 52(11), pp. 2535-2542.

[18] *National Spherical Torus Experiment* (n.d).Wikiwand. https://www.wikiwand.com/en/National_Spherical_Torus_Experiment

[19] Rosen, R. (2018, March 26). *How would Halos affect ITER?.* ITER. https://www.iter.org/newsline/-/2966

[20] McCormack, B., Kaita, R., Kugel, H. & Hatcher, R. (1999). *Rogowski loop designs for NSTX.* 18th IEEE/NPSS Symposium on Fusion Engineering. Symposium Proceedings. pp. 306-309. https://doi.org/10.1109/FUSION.1999.849843.

[21] Delbert, C. (2022, February 17). *El Tokamak más grande del mundo acaba de batir el récord de energía de fusión nuclear.* Esquire. https://www.esquire.com/es/tecnologia/a39120530/record-fusion-nuclear/

[22] Sonato, P., Baker, W.R., Beaumont, P.S., Damiani, C., Fiorentin, P., Guigon, A., Fullard, K., Goodyear, A., Grando, L., Huntley, S.C., Lam, N., Lioure, A., Loving, A., Marcuzzi, D., Mills, S., Peruzzo, S., Pomaro, N., Riccardo, V., & Way, M. (2005). *Status of the halo current sensor project for JET-EP.* Fusion Engineering and Design. 74, pp. 757-761. https://doi.org/10.1016/j.fusengdes.2005.06.230

[23] Madenci, E., & Guven, I. (2015). *The Finite Element Method and Applications in Engineering Using ANSYS®* (2nd ed. 2015.). pp. 15-35. https://doi.org/10.1007/978-1-4899-7550-8

[24] Otero Pereiro, L. L. (2006). *Aprendiendo sobre el Método de los Elementos Finitos* Revista de ingeniería mecánica. 9(3), pp. 7-13, 2006. https://www.redalyc.org/articulo.oa?id=225117945001

[25] Agredano, M., et al. (2021). *Coils and power supply design for the SMall aspect ratio tokamak (SMART).* Fusion Engineering and design 168. https://doi.org/10.1016/j.fusengdes.2021.112683

[26] Mancini, A., et al (2021). *Mechanical and electromagnetic design of the vacuum vessel of the SMART tokamak.* Fusion Enginnering and design 171. https://doi.org/10.1016/j.fusengdes.2021.112542

[27] Mancini, A., et al (2021). *Electromagnetic VDE and disruption analysis in the SMART tokamak.* Fusion Engineering and Design (submitted for publication).

[28] Obrejan, Kevin. (2017). *Study of magnetic shaping effects on plasma flows and micro-instabilities in tokamak plasmas using a full-f gyrokinetic code based on a real space field solver.* (Doctoral thesis, Kyoto University, Kyoto, Japan)

7 GLOSSARY

RC	Rogowski Coil
SMART	Small Aspect Ratio Tokamak
PSFT	Plasma Science and Fusion Technologies
TFC	Toroidal Field Coils
PFC	Poloidal Field Coils